REPORT NO. UMTA-MA-06-0025-80-8

ANALYSIS OF WHEEL/RAIL FORCE AND FLANGE FORCE DURING STEADY STATE CURVING OF RIGID TRUCKS

Herbert Weinstock
Robert Greif

U.S. DEPARTMENT OF TRANSPORTATION
RESEARCH AND SPECIAL PROGRAMS ADMINISTRATION
Transportation Systems Center
Cambridge MA 02142

SEPTEMBER 1980
INTERIM REPORT

Prepared for

U.S. DEPARTMENT OF TRANSPORTATION
URBAN MASS TRANSPORTATION ADMINISTRATION
Office of Technology Development & Deployment
Washington DC 20590

NOTICE

This document is disseminated under the sponsorship of the Department of Transportation in the interest of information exchange. The United States Government assumes no liability for its contents or use thereof.

NOTICE

The United States Government does not endorse products or manufacturers. Trade or manufacturers' names appear herein solely because they are considered essential to the object of this report.

GENERAL DISCLAIMER

This document may be affected by one or more of the following statements

- **This document has been reproduced from the best copy furnished by the sponsoring agency. It is being released in the interest of making available as much information as possible.**
- **This document may contain data which exceeds the sheet parameters. It was furnished in this condition by the sponsoring agency and is the best copy available.**
- **This document may contain tone-on-tone or color graphs, charts and/or pictures which have been reproduced in black and white.**
- **This document is paginated as submitted by the original source.**
- **Portions of this document are not fully legible due to the historical nature of some of the material. However, it is the best reproduction available from the original submission.**

Technical Report Documentation Page

1. Report No.	2. Government Accession No.	3. Recipient's Catalog No.
UMTA-MA-06-0025-80-8		

4. Title and Subtitle	5. Report Date
ANALYSIS OF WHEEL/RAIL FORCE AND FLANGE FORCE DURING STEADY STATE CURVING OF RIGID TRUCKS	September 1980
	6. Performing Organization Code
7. Author(s)	8. Performing Organization Report No.
Herbert Weinstock and Robert Greif	DOT-TSC-UMTA-80-26
9. Performing Organization Name and Address U.S. Department of Transportation Research and Special Programs Administration Transportation Systems Center Cambridge, Massachusetts 02142	10. Work Unit No. (TRAIS) MA-06-0025(UM004/R0746) 11. Contract or Grant No. MA-06-0025
12. Sponsoring Agency Name and Address U.S. Department of Transportation Urban Mass Transportation Administration 400 Seventh Street, S.W. Washington, DC 20590	13. Type of Report and Period Covered Interim Report June 1979-December 1979 14. Sponsoring Agency Code UTD-40

15. Supplementary Notes

16. Abstract Under the Urban Mass Transportation Administration Urban Rail Systems program, the Transportation Systems Center is conducting research and development activities for improving performance and reducing cost of urban rail transit systems. The wheel/rail dynamics interaction project being conducted as part of this program is directed toward reduction of maintenance costs and wheel/rail noise while providing acceptable ride quality and safety. This report describes the development of a simple analysis procedure for estimating the conservative bounds for the wheel/rail forces and flange forces resulting from the curve negotiation of a rigid two-axle truck. The approximate analysis presented provides closed form relations for estimating wheel/rail forces, flange forces, truck angle of attack, and sliding conditions for this type of truck as a function of curve radius. The wheel profiles are modeled by conical wheel treads with vertical wheel flanges and flange friction effects are included. The theory used includes both linear and nonlinear creep and simple suggestions are given for estimating the creep coefficient in a linear theory to obtain results similar to that from a nonlinear theory. The wheel/rail forces produced by curve negotiation of railway vehicles result in wear of both the wheels and rails. In addition, the stick-slip friction characteristics of the frictional component of the wheel/rail forces result in generation of excessive noise in curves. Accordingly, the results of this report can be used in the design and specification of trucks for railroad or transit operations to estimate the wheel/rail interaction forces and slip behavior produced by a truck in curve negotiation. Results of the simplified analysis are compared with test data recently obtained at the Washington Metropolitan Area Transit Authority and are found to be in excellent agreement for cylindrical wheel profiles.

17. Key Words	18. Distribution Statement
Flange Forces; Noise; Railway Vehicles; Transit Car Trucks; Rail Noise; Urban Transit Vehicles; Wheel Noise; Wheel/Rail Forces; Wheel/Rail Noise	Available to the public through the National Technical Information Service, Springfield, Virginia 22161.

19. Security Classif. (of this report)	20. Security Classif. (of this page)	21. No. of Pages	22. Price
Unclassified	Unclassified		

PREFACE

Under the Urban Mass Transportation Administration (UMTA) Urban Rail Systems Program, Transportation Systems Center (TSC) is providing support to the Office of Technology Development and Deployment of the Urban Mass Transportation Administration. Under this program, TSC is responsible for the conduct of research, development and evaluation activities in support of the improvement of urban transit systems. The Wheel/Rail Dynamics Project being conducted as part of this program is directed toward the development of technical data that can be applied to improved performance specifications for transit car trucks and components to permit reductions in maintenance costs and wheel rail noise while providing acceptable ride quality and safety.

The authors would like to thank Ms. Denise Dzwonczyk, a student in the Massachusetts Institute of Technology Mechanical Engineering Department working at TSC under the M.I.T. Engineering Intern Program for her careful review of the equations presented here and for performing the calculations required and plotting the results shown in this paper.

METRIC CONVERSION FACTORS

Approximate Conversions to Metric Measures

Symbol	When You Know	Multiply by	To Find	Symbol
		LENGTH		
in	inches	2.5	centimeters	cm
ft	feet	30	centimeters	cm
yd	yards	0.9	meters	m
mi	miles	1.6	kilometers	km
		AREA		
in^2	square inches	6.5	square centimeters	cm^2
ft^2	square feet	0.09	square meters	m^2
yd^2	square yards	0.8	square meters	m^2
mi^2	square miles	2.6	square kilometers	km^2
	acres	0.4	hectares	ha
		MASS (weight)		
oz	ounces	28	grams	g
lb	pounds	0.45	kilograms	kg
	short tons (2000 lb)	0.9	tonnes	t
		VOLUME		
tsp	teaspoons	5	milliliters	ml
Tbsp	tablespoons	15	milliliters	ml
fl oz	fluid ounces	30	milliliters	ml
c	cups	0.24	liters	l
pt	pints	0.47	liters	l
qt	quarts	0.95	liters	l
gal	gallons	3.8	liters	l
ft^3	cubic feet	0.03	cubic meters	m^3
yd^3	cubic yards	0.76	cubic meters	m^3
		TEMPERATURE (exact)		
°F	Fahrenheit temperature	5/9 (after subtracting 32)	Celsius temperature	°C

Approximate Conversions from Metric Measures

Symbol	When You Know	Multiply by	To Find	Symbol
		LENGTH		
mm	millimeters	0.04	inches	in
cm	centimeters	0.4	inches	in
m	meters	3.3	feet	ft
m	meters	1.1	yards	yd
km	kilometers	0.6	miles	mi
		AREA		
cm^2	square centimeters	0.16	square inches	in^2
m^2	square meters	1.2	square yards	yd^2
km^2	square kilometers	0.4	square miles	mi^2
ha	hectares (10,000 m^2)	2.5	acres	
		MASS (weight)		
g	grams	0.035	ounces	oz
kg	kilograms	2.2	pounds	lb
t	tonnes (1000 kg)	1.1	short tons	
		VOLUME		
ml	milliliters	0.03	fluid ounces	fl oz
l	liters	2.1	pints	pt
l	liters	1.06	quarts	qt
l	liters	0.26	gallons	gal
m^3	cubic meters	35	cubic feet	ft^3
m^3	cubic meters	1.3	cubic yards	yd^3
		TEMPERATURE (exact)		
°C	Celsius temperature	9/5 (then add 32)	Fahrenheit temperature	°F

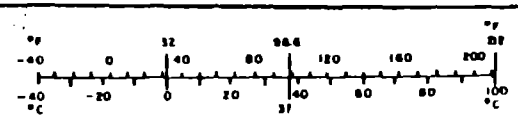

TABLE OF CONTENTS

LIST OF ILLUSTRATIONS

LIST OF TABLES

NOMENCLATURE

f = creep coefficient (linear theory)

f^* = creep coefficient (nonlinear theory)

F = lateral force

F_g = lateral flange force

h = ratio of wheel base to track gauge

ℓ = half of track gauge

M = moment

N = normal force on wheel

P = net lateral (centrifugal) force

q = half of total flange clearance

r = wheel radius of displaced wheelset

r_o = wheel radius of undisplaced wheelset

R = curve radius

V = truck velocity

W = total load

y = lateral displacement

α = wheel conicity

β, γ = orientation of resultant velocity on leading and trailing wheels

δ = alignment deviation of irregular track

μ = wheel/rail coefficient of friction

μ_F = flange coefficient of friction

ψ = yaw angle of truck with normal to curve

Subscripts

L = lateral

R = resultant

T = tangential

1,2 = trailing and leading axle, respectively.

EXECUTIVE SUMMARY

Under the UMTA Urban Rail Systems Program, TSC is conducting research and development activities for improving performance and reducing cost of urban rail transit systems. The Wheel/Rail Dynamics Interaction Project being conducted as part of this program is directed toward reduction of maintenance costs and wheel rail noise while providing acceptable ride quality and safety. This report describes the development of a simple analysis procedure for estimating the steady state forces produced by a rigid truck in curve negotiation. The rigid truck analysis presented here for a two-axle truck provides a conservative upper bound on the wheel rail and flange forces that could be expected for actual truck designs under steady curving conditions. The closed form analytic relationships provided for estimating forces, truck angle of attack, and slip conditions as a function of curve radius also permit a simple check on the validity of more complex analytical models of truck designs and associated computer programs for predicting wheel rail forces and kinematics. This analysis idealizes the wheel profile as a tread with constant conicity with a vertical wheel flange. The analysis includes both linear and nonlinear creep theory. The effects of creep force saturation and wheel sliding on wheel rail forces and flange forces are presented. The range of validity of the rigid truck approximation is defined by comparison of the results with those predicted by more complete (but more complicated) analyses including truck flexibility. Results of the simplified analysis are compared with test data recently obtained at the Washington Metropolitan Area Transit Authority and are found to be in excellent agreement for cylindrical wheel profiles.

1. INTRODUCTION

The wheel rail forces produced by curve negotiation of railway vehicles result in wear of both the wheels and rails. In addition, the stick-slip friction characteristics of the frictional component of the wheel/rail forces result in generation of excessive noise in curves. Accordingly, in the design and specification of trucks for railroad or transit operations it is important to estimate the wheel/rail interaction forces and slip behavior produced by a truck in curve negotiation.

Previous investigation of steady state curve mechanics includes the work of Newland [1] and Boocock [2]. These papers include analyses of both rigid and flexible trucks and gross slipping of wheels but do not include the effects of flanging. The relationship between creep and conicity for steering a truck through a curve is explored in these papers. Other investigators have used a steady state friction center model to study the curving problem and have included flange force behavior in their calculations. Graphical procedures based on this technique include the work of Porter and Muller, and some examples are given by Koffman [3]. Iterative numerical techniques that include nonlinear effects such as creep and clearances have been established by Koci and Marta [4].

An overview of computational methods for the prediction of truck performance in curves is given by Perlman [5] and includes a list of applicable references. Elkins and Gostling [6] investigated the curving behavior of a wheelset including nonlinearities in contact geometry and creep characteristics. Computer solutions are obtained and no closed form results are presented.

Several computer programs have been developed for analysis of the steady state curving problem, for the Department of Transportation including Battelle SSCUR under DOT-TSC-1051 [7] and the work of Law under DOT-TSC-902, which take into account details of truck suspension and car design. These programs, however, require detailed knowledge of the car and truck design parameters which normally would not be available for a first estimate.

This report presents closed form analytic solutions for the mechanics of curve negotiation which include the effects of flanging. Conservative bounds for the wheel/rail forces and slip motions are obtained from the analysis of rigid frame trucks. An analysis is presented of a two-axle rigid frame truck which provides closed form relationships for estimating the wheel/rail forces, angle of attack and sliding conditions produced by this type of truck as a function of curve radius. In this paper the wheel profiles are modeled by conical wheel treads with vertical wheel flanges and it is assumed that the flange is perfectly lubricated. It is shown that the effect of friction between the vertical flange and the rail is to reduce the flange force. These models and assumptions should provide a good approximation for cases where wheel climb does not dominate the solution.

Analyses are presented to assess the applicability of this rigid truck model to a flexible truck design with interaction between axles through elastic members. For a flexible truck modeled by lateral and longitudinal primary stiffness connected to the frame, relationships are derived in terms of the effective inter-axle stiffnesses.

Inequalities are derived to define the rigid and flexible truck range in terms of these primary stiffnesses. A comparison of the rigid truck results with test data for consists of the Washington Metropolitan Area Transit Authority is presented. For trucks equipped with cylindrical wheels, the comparison of wheel/rail force levels between the rigid truck model and the experimental results is excellent.

2. TRUCK FORCES

Forces act on the truck to produce the deviations from pure rolling motion required for curve negotiation. The creep velocity is the difference between the actual velocity and the velocity predicted for a pure rolling condition. For small creep velocity, the creep forces are approximately proportional to the creep velocity. For large lateral displacements of the wheel, the truck cannot traverse the curve without flanging. In this section, a method is presented for the calculation of the flange forces of a rigid truck in which the wheels are idealized to have constant conicity and vertical flanges and it is assumed that the flange is perfectly lubricated. Upon saturation of the creep force and initiation of wheel slip, force levels are limited by the value of the coefficient of friction.

Using the velocity components shown in Figure 1, the lateral and tangential creep velocities are

$$V_{L1} = \dot{y}_1 - V\psi \tag{1}$$

$$V_{L2} = \dot{y}_2 - V\psi$$

$$V_{T_{1i}} = V\left(\frac{r_{1i}}{r_o} - 1\right) + \ell\,(\dot{\phi} + \dot{\psi})$$

$$V_{T_{2i}} = V\left(1 - \frac{r_{2i}}{r_o}\right) + \ell\,(\dot{\phi} + \dot{\psi})$$

where the first subscript corresponds to the wheel number with the outboard wheel designated by 1 and the inboard wheel designated by 2. The second subscript corresponds to the axle number with the trailing axle designated by 1 and the leading axle designated by 2. The change in rolling radius with lateral displacement is

$$r_{1i} = r_o + \alpha\,(y_i - \delta_{1i}) \tag{2}$$

$$r_{2i} = r_o - \alpha\,(y_i - \delta_{2i}).$$

Where the δ terms correspond to alignment deviation of irregular track. For steady state curving

$$\dot{\phi} = \frac{-V}{R}\,,\quad \dot{\psi} = 0\,,\quad \dot{y} = 0. \tag{3}$$

The rigid body kinematic relations for y_1 and y_2, the lateral displacements for axles 1 and 2, are

$$y_1 = y - h\ell\psi \qquad\qquad y_2 = y + h\ell\psi \tag{4a}$$

and the lateral velocity terms are

$$\dot{y}_1 = \frac{h\ell V}{R} \qquad\qquad \dot{y}_2 = -\frac{h\ell V}{R}. \tag{4b}$$

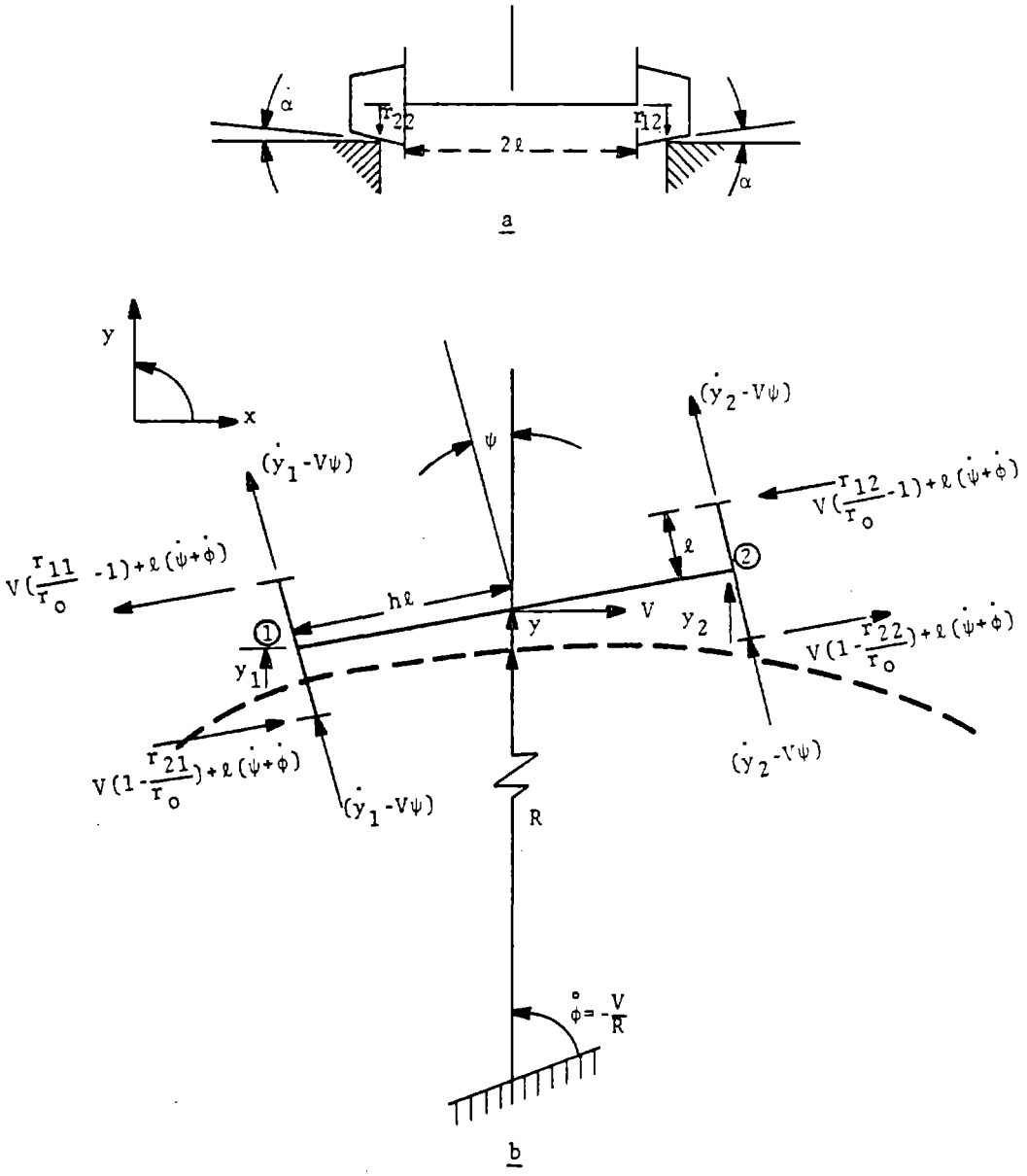

FIGURE 1. STEADY STATE CURVING MODEL OF RIGID TWO-AXLE TRUCK SHOWING CREEP VELOCITY COMPONENTS

Substituting the relations from (2) - (4) into (1) leads to the creep velocities for this steady state curving condition

$$V_{L_1} = V\left(\frac{h\ell}{R} - \psi\right) \qquad V_{L_2} = -V\left(\frac{h\ell}{R} + \psi\right)$$

$$V_{T_{1i}} = V\left(\frac{\alpha}{r_o} y_i - \frac{\ell}{R}\right) - \frac{V\alpha}{r_o}\delta_{1i} \tag{5}$$

$$V_{T_{2i}} = V\left(\frac{\alpha}{r_o} y_i - \frac{\ell}{R}\right) - \frac{V\alpha}{r_o}\delta_{2i},$$

The force acting on each wheel is composed of creep forces proportional to the creep velocities of equation (5), gravitational forces associated with wheel conicity and also possible flange forces, Fg, as depicted in Figure 2. The lateral axle forces on each of the two axles are given by (neglecting spin creep effects)

$$F_1 = -2f_L\left(\frac{h\ell}{R} - \psi\right) + Fg_1 \quad \text{(trailing)} \tag{6}$$

$$F_2 = 2f_L\left(\frac{h\ell}{R} + \psi\right) + Fg_2 \quad \text{(leading)}$$

where f_L is the lateral creep coefficient. The moment on each axle is given by

$$M_1 = -2f_T\ell\left[\frac{\alpha}{r_o}(y - h\ell\psi) - \frac{\ell}{R}\right] + \frac{2f_T\,\alpha\,\ell\bar{\delta}_1}{r_o} \quad \text{(trailing)} \tag{7}$$

$$M_2 = -2f_T\ell\left[\frac{\alpha}{r_o}(y + h\ell\psi) - \frac{\ell}{R}\right] + \frac{2f_T\,\alpha\,\ell\bar{\delta}_2}{r_o} \quad \text{(leading)}$$

where f_T is the tangential creep coefficient and $\bar{\delta}_1$ and $\bar{\delta}_2$ correspond to the location of the track centerline for axles 1 and 2,

$$\bar{\delta}_1 = \frac{\delta_{11} + \delta_{21}}{2}, \quad \bar{\delta}_2 = \frac{\delta_{12} + \delta_{22}}{2}. \tag{8}$$

Assuming that the truck is subjected to a new lateral force P, the total lateral truck force is

$$F_1 + F_2 + P = 0 \tag{9}$$

$$4f_L\psi + (Fg_1 + Fg_2) + P = 0.$$

Assuming zero centerplate friction, which is a good approximation for most modern transit trucks, the total moment on the truck is zero,

$$M_1 + M_2 + (F_2 - F_1)\,h\ell = 0 \tag{10}$$

$$4f_T\ell\left(\frac{\ell}{R} - \frac{\alpha}{r_o}\left\{y - \frac{\bar{\delta}_1 + \bar{\delta}_2}{2}\right\}\right) + 4f_L\frac{h^2\ell^2}{R} + (Fg_2 - Fg_1)\,h\ell = 0.$$

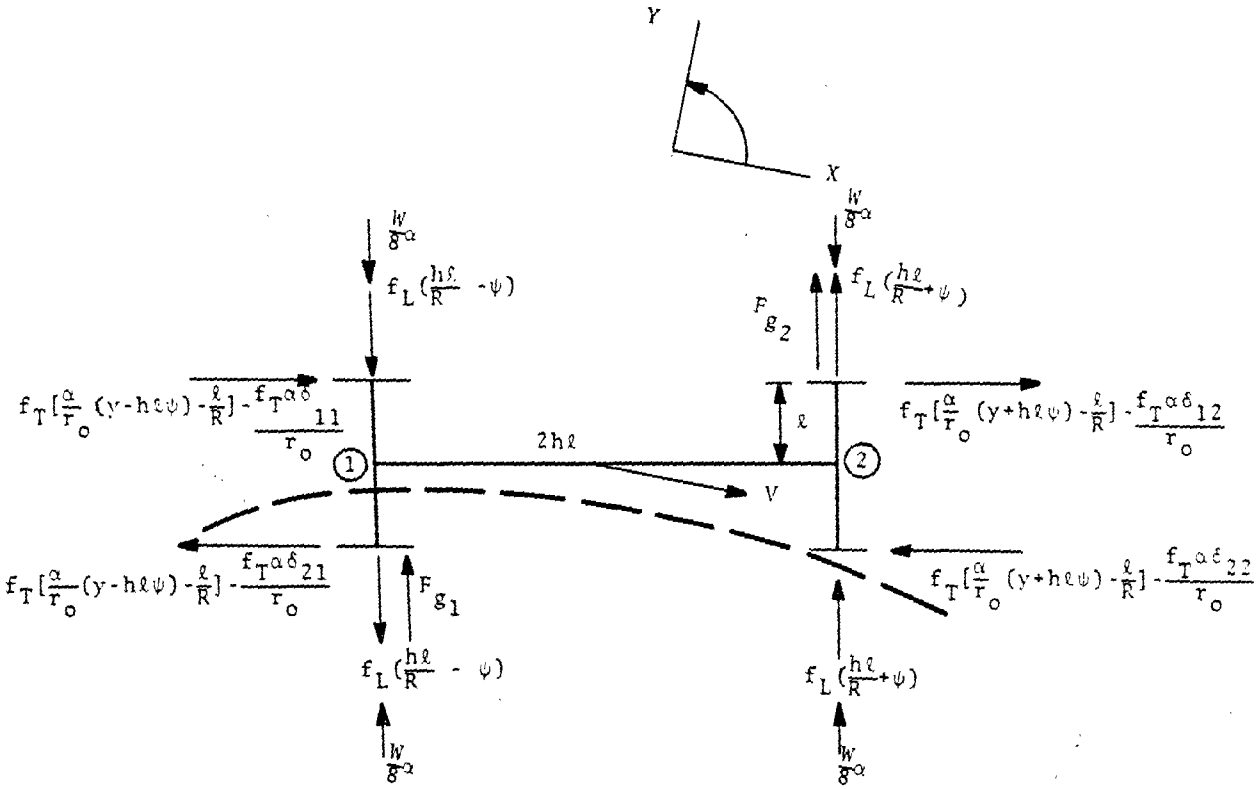

FIGURE 2. TRUCK FORCES

Assuming, as a first approximation, that the tangential and lateral creep coefficients are equal (i.e., $f_T = f_L = f$) and introducing the relative displacement y_a

$$y_a = y - \frac{\bar{\delta}_1 + \bar{\delta}_2}{2} \tag{11}$$

the relationships from (9) and (10) may be solved simultaneously for the flange forces Fg_1 and Fg_2 as follows

$$Fg_2 = \frac{-2f}{h}\left[\frac{(1+h^2)\ell}{R} - \frac{\alpha y_a}{r_o}\right] - 2f\psi - \frac{P}{2} \tag{12}$$

$$Fg_1 = \frac{2f}{h}\left[\frac{(1+h^2)\ell}{R} - \frac{\alpha y_a}{r_o}\right] - 2f\psi - \frac{P}{2}.$$

CURVING REGIONS

Wheel/rail forces and associated truck geometry are developed for the three curving regions. These regions are creep guidance (no flanging), free curving (flanging on lead outer wheel) and constrained curving (flanging on lead outer wheel and trailing inner wheel). It is assumed that the force levels produced are such that gross sliding (slipping) does not occur. In the next section the effects of adhesion level and gross sliding are considered.

Creep Guidance Region

In this region the truck is guided totally by the wheel conicity and creep forces with no flange contact. Setting $Fg_1 = Fg_2 = 0$ in equation (12) and solving for yaw angle ψ and relative lateral displacement y_a, yields

$$\psi = -\frac{P}{4f},\quad y_a = (1+h^2)\left(\frac{r_o\ell}{\alpha R}\right). \tag{13}$$

The lateral axle forces are then found from equation (6) as

$$F_1 = -2f((h\ell/R) + P/4f) \tag{14}$$

$$F_2 = 2f((h\ell/R) - P/4f).$$

The wheel rail lateral forces are obtained from Figure 2, after substituting in the yaw angle and zero flange force. The terminology "inward" defines a force on the wheel toward the center of curvature while the terminology "outward" defines a force on the wheel away from the center of curvature,

$$\text{leading axle outboard} = f\left(\frac{h\ell}{R} - \frac{P}{4f}\right) - \frac{W}{8}\alpha \tag{15}$$

$$\text{leading axle inboard} = f\left(\frac{h\ell}{R} - \frac{P}{4f}\right) + \frac{W}{8}\alpha$$

$$\text{trailing axle outboard} = -f\left(\frac{h\ell}{R} + \frac{P}{4f}\right) - \frac{W}{8}\alpha \text{ (inward)}$$

$$\text{trailing axle inboard} = -f\left(\frac{h\ell}{R} + \frac{P}{4f}\right) + \frac{W}{8}\alpha.$$

The minimum curve radius that can be negotiated without flange contact is found from equation (12) by setting $y_a = q - h\ell\psi$, where q is half of the total flange clearance, (see equation (17)),

$$R \geq \frac{(1 + h^2)\, r_o \ell}{\alpha\left(q + \frac{h\ell^2}{4f}\right)} . \tag{16}$$

"Free" Curving Region

In this region the truck is guided by a combination of the creep forces and a flange force at the outboard wheel of the leading axle; there is no flanging on the wheels of the trailing axle. The maximum lateral displacement that axle 2 can incur is q. The relative displacement y_a is then

$$y_2 = q \tag{17}$$

$$y_a = q - h\ell\psi .$$

Using $Fg_1 = 0$ in equation (12) leads to a yaw angle ψ consistent with equation (17).

$$\psi = \frac{(1 + h^2)\,\frac{\ell}{R} - \frac{\alpha q}{r_o} - \frac{Ph}{4f}}{h\left(1 - \frac{\alpha\ell}{r_o}\right)} \tag{18}$$

$$\psi_{max} = \frac{q}{h\ell}$$

where the maximum yaw angle of $q/h\ell$ follows from equation (17) by setting $y_a = 0$. Equation (18) shows that the effect of centrifugal force is to reduce the angle of attack. The flange force of the outboard wheel of the leading axle Fg_2 is derived from equation (12) by adding the relations together and using $Fg_1 = 0$,

$$Fg_2 = -4f\psi - P \quad \text{(inward)} \tag{19}$$

$$= -4f\left[\frac{(1 + h^2)\,\frac{\ell}{R} - \frac{\alpha q}{r_o}}{h\left(1 - \frac{\alpha\ell}{r_o}\right)}\right] + \frac{P(\alpha\ell/r_o)}{1 - \frac{\alpha\ell}{r_o}} .$$

This result shows that for a cylindrical wheel, $\alpha = 0$, the flange force is independent of the centrifugal force P. For conical wheels, the effect of the centrifugal force is to reduce the flange force Fg_2. The lateral wheel rail forces are obtained from Figure 2, using the flange force from equation (19),

$$\text{leading axle outboard} = F_{g_2} + f\left(\frac{h\ell}{R} + \psi\right) - \frac{W}{8}\alpha \tag{20}$$

$$= \frac{3}{4}F_{g_2} + \frac{fh\ell}{R} - \frac{P}{4} - \frac{W}{8}\alpha$$

$$\text{leading axle inboard} = f\left(\frac{h\ell}{R} + \psi\right) + \frac{W}{8}\alpha$$

$$= -\frac{1}{4}F_{g_2} + \frac{fh\ell}{R} - \frac{P}{4} + \frac{W}{8}\alpha$$

$$\text{trailing axle outboard} = -f\left(\frac{h\ell}{R} - \psi\right) - \frac{W}{8}\alpha$$

$$= -\frac{1}{4}F_{g_2} - \frac{fh\ell}{R} - \frac{P}{4} - \frac{W}{8}\alpha$$

$$\text{trailing axle inboard} = -f\left(\frac{h\ell}{R} - \psi\right) + \frac{W}{8}\alpha$$

$$= -\frac{1}{4}F_{g_2} - \frac{fh\ell}{R} + \frac{P}{4} + \frac{W}{8}\alpha .$$

This shows that for the free curving region the centrifugal force is reacted equally on all four wheels. The maximum radius applicable to this free curving region is set by equation (16) and the minimum radius is determined by setting $\psi = \psi_{max}$ in equation (18) so that

$$\frac{(1 + h^2)\ell}{\left(\frac{q}{\ell} + \frac{Ph}{4f}\right)} < R < \frac{(1+h^2)\, r_o}{\alpha\left(\frac{q}{\ell} + \frac{Ph}{4f}\right)} . \tag{21}$$

Constrained Curving Region

In this region the truck is guided by the combination of creep forces and flanging on two wheels. Both the outboard wheel of the leading axle and the inboard wheel of the trailing axle are flanging and tending to widen the track gauge. The yaw angle reaches its maximum value, ψ_{max} and the relative displacement y_a is zero,

$$\psi = \psi_{max} \tag{22}$$

$$= q/h\ell .$$

The flange forces are then found from equation (12)

$$F_{g_2} = \frac{-2f}{h}\left[(1+h^2)\,\frac{\ell}{R} + \frac{q}{\ell}\right] - \frac{P}{2}$$

$$F_{g_1} = \frac{2f}{h}\left[(1+h^2)\,\frac{\ell}{R} - \frac{q}{\ell}\right] - \frac{P}{2} . \tag{23}$$

The lateral wheel rail forces are obtained from Figure 2 by substituting the flange forces from equation (23) and ψ_{max} from equation (22),

$$\text{leading axle outboard} = F_{g_2} + f\left(\frac{h\ell}{R} + \frac{q}{h\ell}\right) - \frac{W}{8}\alpha$$

$$\text{leading axle inboard} = f\left(\frac{h\ell}{R} + \frac{q}{h\ell}\right) + \frac{W}{8}\alpha \tag{24}$$

$$\text{trailing axle outboard} = f\left(-\frac{h\ell}{R} + \frac{q}{h\ell}\right) - \frac{W}{8}\alpha$$

$$\text{trailing axle inboard} = F_{g_1} + f\left(-\frac{h\ell}{R} + \frac{q}{h\ell}\right) + \frac{W}{8}\alpha .$$

Due to the utility of this force and geometry data, the results for all three curving regions have been summarized in Table 1. The limitations inherent in these results should be noted: a vertical flange model has been used, a linear creep model and no gross sliding has been included. The effects of non-linear creep and gross sliding (force saturation) have been included in a later part of this paper.

TABLE 1. CURVING REGIONS (NO GROSS SLIDING)

REGION	RADIUS	FLANGE FORCES	WHEEL RAIL LATERAL FORCES (acting on truck)
Constrained Curving	$R<R_1$ $R_1 = \frac{(1+h^2)\ell}{\left(\frac{q}{\ell} + \frac{Ph}{4f}\right)}$	$F_{g_2} = -\frac{2f}{h}\left[(1+h^2)\frac{\ell}{R} + \frac{q}{\ell}\right] - \frac{P}{2}$ $F_{g_1} = \frac{2f}{h}\left[(1+h^2)\frac{\ell}{R} - \frac{q}{\ell}\right] - \frac{P}{2}$	leading axle outboard = $F_{g_2} + f\left(\frac{h\ell}{R} + \frac{q}{h\ell}\right) - \frac{W}{8}\alpha$ leading axle inboard = $f\left(\frac{h\ell}{R} + \frac{q}{h\ell}\right) + \frac{W}{8}\alpha$ trailing axle outboard= $f\left(\frac{-h\ell}{R} + \frac{q}{h\ell}\right) - \frac{W}{8}\alpha$ trailing axle inboard = $F_{g_1} + f\left(-\frac{h\ell}{R} + \frac{q}{h\ell}\right) + \frac{W}{8}\alpha$
Free Curving	$R_1 \leq R \leq R_o$ $R_o = \frac{(1+h^2)\ r_o}{\alpha\left(\frac{q}{\ell} + \frac{Ph}{4f}\right)}$	$F_{g_2} = -4f\left(\frac{(1+h^2)\frac{\ell}{R} - \frac{\alpha q}{r_o}}{h\left(1-\frac{\alpha\ell}{r_o}\right)}\right) + \frac{P(\alpha\ell/r_o)}{1-\frac{\alpha\ell}{r_o}}$ $F_{g_1} = 0$	leading axle outboard = $\frac{3}{4}F_{g_2} + f\frac{h\ell}{R} - \frac{P}{4} - \frac{W}{8}\alpha$ leading axle inboard = $-\frac{1}{4}F_{g_2} + f\frac{h\ell}{R} - \frac{P}{4} + \frac{W}{8}\alpha$ trailing axle outboard= $-\frac{1}{4}F_{g_2} - f\frac{h\ell}{R} - \frac{P}{4} - \frac{W}{8}\alpha$ trailing axle inboard = $-\frac{1}{4}F_{g_2} - f\frac{h\ell}{R} - \frac{P}{4} + \frac{W}{8}\alpha$
Creep Guidance	$R \geq R_o$	$F_{g_2} = 0$ $F_{g_1} = 0$	leading axle outboard = $f\frac{h\ell}{R} - \frac{P}{4} - \frac{W}{8}\alpha$ leading axle inboard = $f\frac{h\ell}{R} - \frac{P}{4} + \frac{W}{8}\alpha$ trailing axle outboard= $-f\frac{h\ell}{R} - \frac{P}{4} - \frac{W}{8}\alpha$ (inward) trailing axle inboard = $-f\frac{h\ell}{R} - \frac{P}{4} + \frac{W}{8}\alpha$

3. NUMERICAL CALCULATIONS

As an illustration of the previously derived relationships, several numerical values are derived for the following typical truck values,

$$\ell = 2.35' \qquad \alpha = 1/20 \qquad h = 1.41$$
$$r_o = 1.25' \qquad q = .0338' \tag{25}$$

For the following numerical calculations it is assumed that the steady state curving motion is taking place at balance speed, so that the net lateral force P is taken as zero. Following Table 1, the limiting curve radius for each curving region is,

$$\begin{aligned} &\text{constrained curving:} && R < 490 \text{ feet}, \ \psi_{max} = .584^\circ \\ &\text{free curving:} && 490 \text{ feet} < R < 5214 \text{ feet} \\ &\text{creep guidance:} && R > 5214 \text{ feet}. \end{aligned} \tag{26}$$

In order to derive first order values for the forces, an estimate of the creep coefficient is needed. An approximate value for the creep coefficient in the linear range is about 150 times the wheel load. Since we are dealing with large creep, a value of about 75 times the normal force is probably more appropriate. (Further discussion of the accuracy of these values can be found in the section on non-linear creep.) The creep coefficient, assuming a 100,000# car weight with two trucks and an equal weight distribution, is then

$$\begin{aligned} f &= \frac{75W}{8} \\ &= 9.375 \times 10^5 \ \#. \end{aligned} \tag{27}$$

Consider the free curving case with a 850 foot radius curve. The flanging wheel on the lead axle has a flange force

$$\begin{aligned} F_{g_2} &= -4f\left[\frac{(1+h^2)\frac{\ell}{R} - \frac{\alpha q}{r_o}}{h\left(1 - \frac{\alpha\ell}{r_o}\right)}\right] \\ &= -20{,}282\# \end{aligned} \tag{28}$$

where the minus sign implies that this force acts on the truck, toward the center of curvature. The <u>lead</u> axle wheel rail forces are found (using Table 1),

$$\begin{aligned} \text{outboard force} &= \tfrac{3}{4}F_{g_2} + f\frac{h\ell}{R} - \frac{W}{8}\alpha \\ &= -12{,}182\# \text{ (inward)} \end{aligned} \tag{29}$$

$$\begin{aligned} \text{inboard force} &= -\tfrac{1}{4}F_{g_2} + f\frac{h\ell}{R} + \frac{W}{8}\alpha \\ &= +9{,}350\# \text{ (outward)} \end{aligned} \tag{30}$$

the trailing axle, wheel rail forces are

$$\text{outboard force} \left\{ = -\frac{1}{4} F_{g_2} - \frac{fh\ell}{R} + \frac{W}{8} \right.$$
$$\text{inboard force} \left\{ = 791\# \text{ (outboard)}, \ 2041\# \text{ (inboard)}. \right. \tag{31}$$

The lateral forces for this free curving region are shown on Figure 3. (The forces in Figure 3 enclosed with parentheses correspond to the forces for the slipped condition with $\mu = 1/2$. These forces will be discussed in the next section on "Slipped Conditions".) As shown in Figure 3, the lead axle forces act to widen the gauge while the trailing axle forces act to push the rail inward. The maximum friction force the wheels can develop is μN where μ is the coefficient of friction. For the 100,000 lb. car, N = 12,500 and for $\mu = 0.5$, the maximum force would be 6,250 lb. The predicted forces for the trailing axle are well within this limiting friction value, however, the predicted 9,350 lb force would require a coefficient of friction of about 0.7. It is therefore believed the above represents a high estimate, with forces that would be developed on very clean dry rail.

The relationship among flange, wheel/rail force and curving regions are shown in Figures 4-6 based on the values tabulated in Table 1. Note that the force levels are linearly proportional to the curvature (1/R), assuming that sliding has not occurred. From equation (16) the minimum curve radius negotiable without flange contact is 5190 feet for the rigid truck and 1738 feet for the single axle wheelset. From Figures 4 and 5, it may be seen that the lead axle cannot enter the constrained curving region without gross sliding occurring. A comparison of Figures 5 and 6 shows that in the free curving region (flanging on lead outer wheel) the wheel/rail forces for leading axle are much greater than the corresponding forces for the trailing axle. The flange force on the outboard wheel of the leading axle can become quite high before sliding occurs reaching 14,000# ($\mu = 1/2$) and 29,000# ($\mu = 1$).

SLIP CONDITIONS

The previous results will hold only for the case of no wheel slipping. However, the maximum value that the resultant force can acquire is μN, where μ is the friction coefficient and N is the wheel load. It is assumed that once a wheel slips, the resultant force is aligned with the resultant creep velocity. Typically the lead axle will slip before the trailing axle. Two cases are considered in this section; in the first case the lead axle slips and the trailing axle does not slip while in the second case both axles slip.

Lead Axle Slipping, Trailing Axle Not Slipping

The creep velocities for the wheels of the lead axle are given in equation (5)

$$V_{L_2} = -V \left(\frac{h\ell}{R} + \psi \right) \tag{32a}$$
$$V_{T_2} = V \left(\frac{\alpha}{r_o} \left\{ y + h\ell\psi \right\} - \frac{\ell}{R} \right)$$

and the direction of the resultant velocity vector is governed by

$$\tan \beta = V_{L_2} / V_{T_2}. \tag{32b}$$

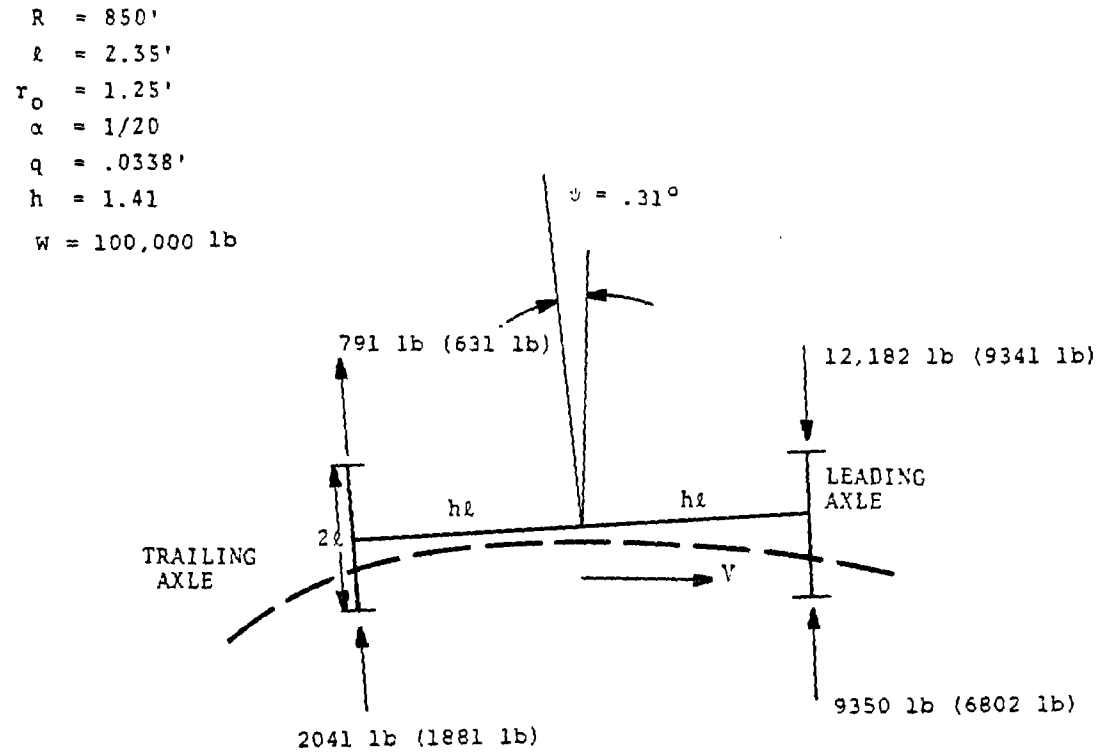

FIGURE 3. APPROXIMATE LATERAL FORCE LEVELS ON TRUCK FOR FREE CURVING REGION WITH 850' RADIUS (THE FORCES IN PARENTHESES CORRESPOND TO SLIPPED CONDITIONS WITH $\mu = 1/2$)

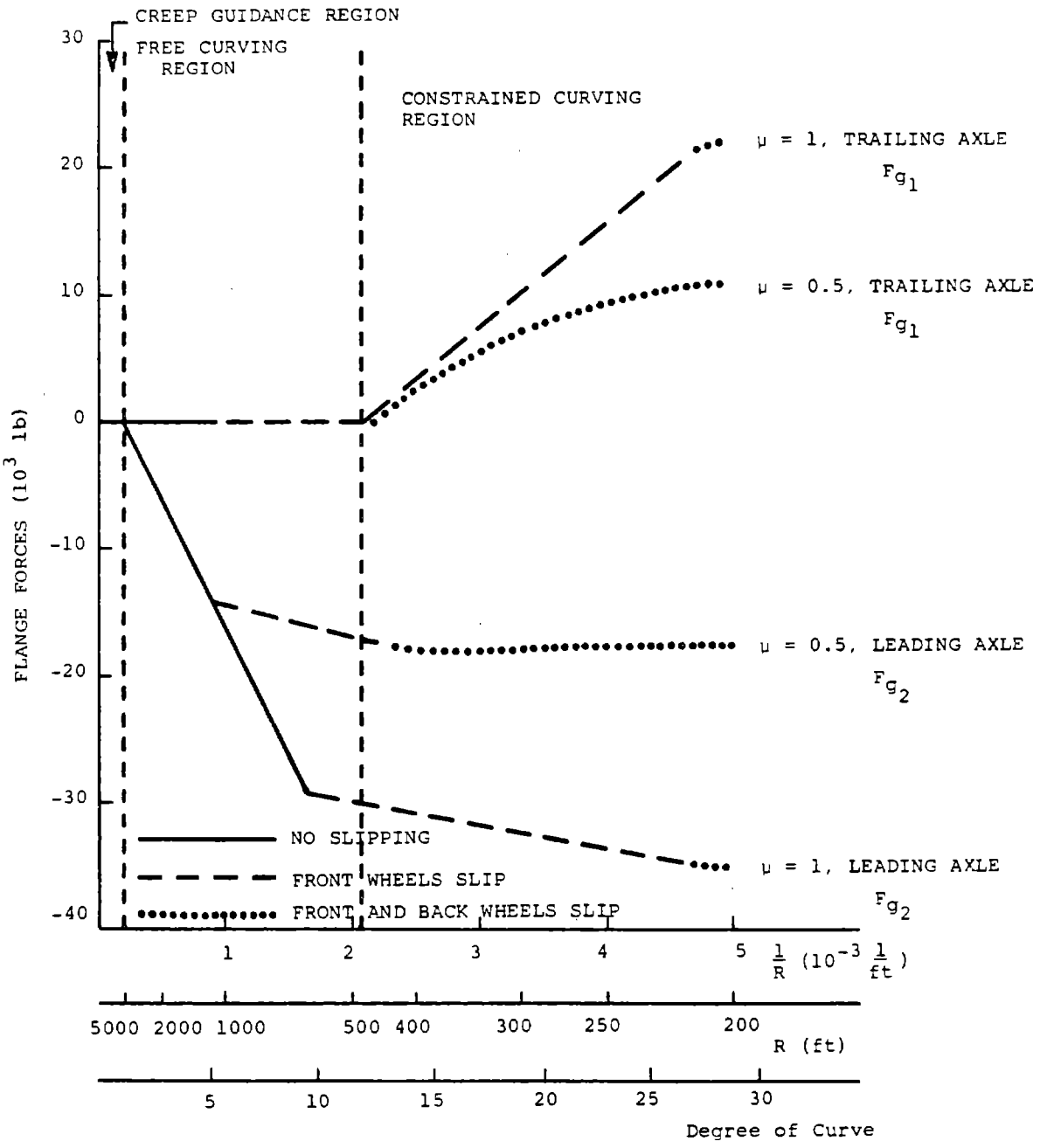

FIGURE 4. FLANGE FORCE ON INNER AND OUTER AXLE VERSUS RADIUS OF TRACK

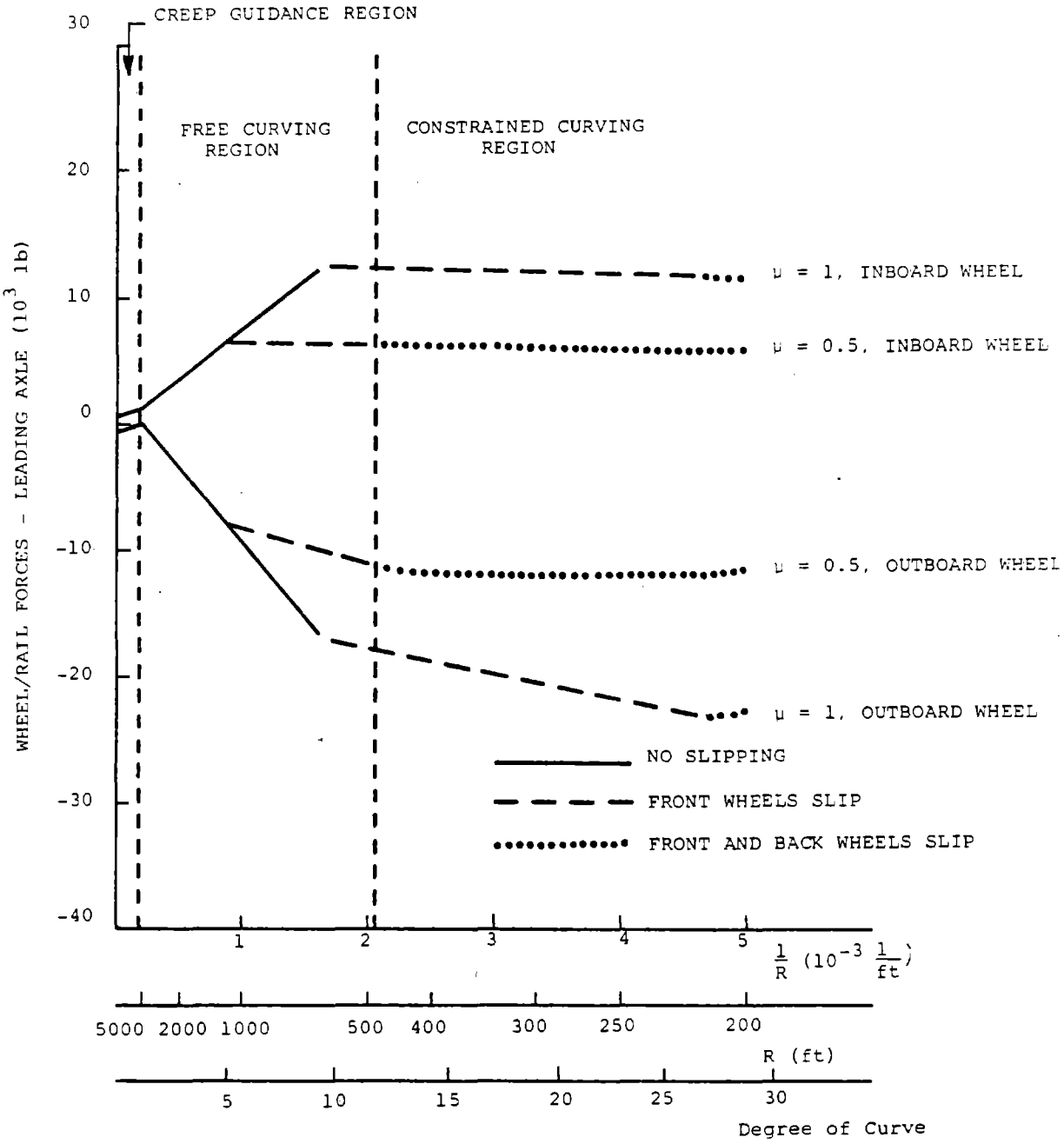

FIGURE 5. LATERAL WHEEL/RAIL FORCES ON LEADING AXLE VERSUS RADIUS OF TRACK

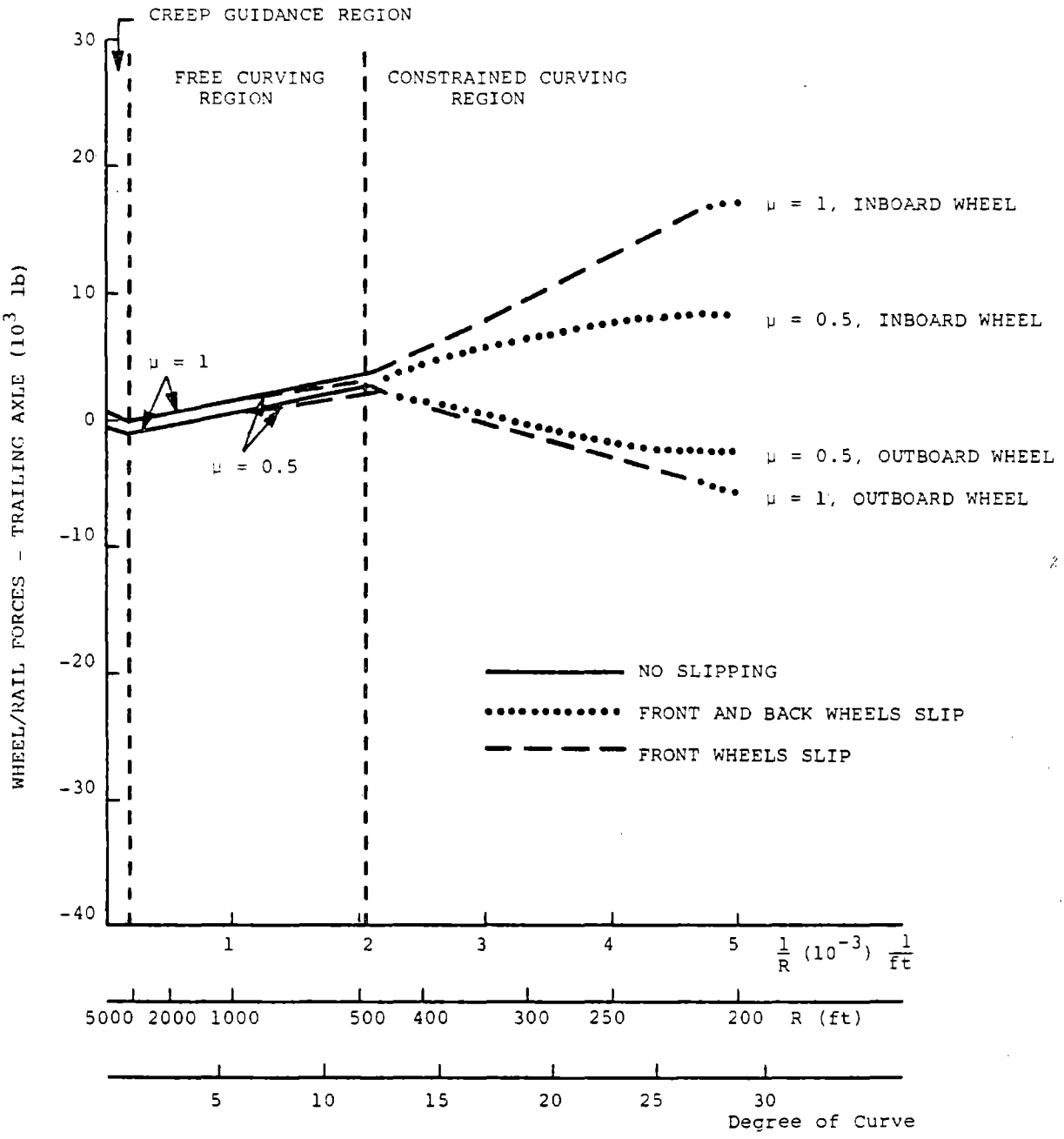

FIGURE 6. LATERAL WHEEL/RAIL FORCES ON TRAILING AXLE VERSUS RADIUS OF TRACK

In these expressions, the alignment deviation terms δ have been omitted for simplicity of analysis and P is taken to be zero. The lateral forces on the two axles follow from equation (6) and the saturation of the resultant creep force is μN.

$$F_1 = -2f\left(\frac{h\ell}{R} - \psi\right) + F_{g_1} \qquad \text{trailing}$$

$$F_2 = 2\mu N \sin\beta + F_{g_2} \qquad \text{leading, slipping} \tag{33a}$$

and the corresponding moments on the axles are

$$M_1 = -2f\ell\left[\frac{\alpha}{r_o}(y - h\ell\psi) - \frac{\ell}{R}\right]$$

$$M_2 = 2\ell\mu N\cos\beta \tag{33b}$$

Setting the total lateral force to zero and the total truck moment to zero leads to two equations which provide explicit expressions for the flange forces F_{g_1} and F_{g_2}

$$F_{g_2} = -2\mu N\sin\beta - \frac{\mu N}{h}\cos\beta + \frac{f}{h}\left[\frac{\alpha}{r_o}(y - h\ell\psi) - \frac{\ell}{R}\right] \tag{34a}$$

$$F_{g_1} = 2f\left(\frac{h\ell}{R} - \psi\right) + \frac{\mu N}{h}\cos\beta - \frac{f}{h}\left[\frac{\alpha}{r_o}(y - h\ell\psi) - \frac{\ell}{R}\right], \tag{34b}$$

If the lead axle slippage occurs in the <u>free curving region</u>, associated with flanging at the outboard wheel of the lead axle,

$$y_2 = q \quad , \quad y = q - h\ell\psi$$

$$F_{g_1} = 0. \tag{35}$$

then the yaw angle ψ is found upon substitution of the relations from (35) into equation (34b),

$$\psi = \frac{\frac{\ell}{R}(1+2h^2) - \frac{\alpha q}{r_o} + \frac{\mu N}{f}\cos\beta}{2h\left(1 - \frac{\alpha\ell}{r_o}\right)}, \tag{36}$$

Although this equation is transcendental, with β defined by equation (32b) it is relatively simple to solve since β varies slowly with ψ. Substitution of the yaw angle into (34a) yields a value for the flange force F_{g_2} while the axle forces are found from (33a).

If the lead axle slippage occurs in the <u>constrained curving region</u>, associated with flanging at both the lead outer wheel and the trailing inner wheel, where

$$\psi = \psi_{max} \quad , \quad y = 0$$

$$= q/h\ell \tag{37}$$

then the flange forces are found by substitution of (37) into (34),

$$F_{g_2} = -2\mu N\sin\beta - \frac{\mu N}{h}\cos\beta - \frac{f}{h}\left[\frac{\alpha q}{r_o} + \frac{\ell}{R}\right]$$

$$F_{g_1} = 2f\left(\frac{h\ell}{R} - \frac{q}{h\ell}\right) + \frac{\mu N}{h}\cos\beta + \frac{f}{h}\left[\frac{\alpha q}{r_o} + \frac{\ell}{R}\right]. \tag{38}$$

The axle forces F_1 and F_2 follow from substitution of these flange force values into equation (33a).

Both Lead Axle and Trailing Axle Slipping

In this region, the resultant force on the wheels of both the lead and trailing axles reaches saturation levels, and the lateral axle forces can be written as

$$F_1 = 2\mu N\sin\gamma + F_{g_1}$$

$$F_2 = 2\mu N\sin\beta + F_{g_2} \tag{39a}$$

where

$$\tan\gamma = V_{L_1}/V_{T_1} \tag{39b}$$

and the creep velocities on the wheels of the trailing axles are defined in equation (5). The corresponding moments on the axles are given by

$$M_1 = 2\ell\mu N\cos\gamma$$

$$M_2 = 2\ell\mu N\cos\beta. \tag{40}$$

Setting the total lateral force to zero and the total truck moment to zero leads to two equations which can be solved for explicit expressions for the flange forces F_{g_1} and F_{g_2},

$$F_{g_2} = -2\mu N\sin\beta - \frac{\mu N}{h}(\cos\beta + \cos\gamma) \tag{41a}$$

$$F_{g_1} = -2\mu N\sin\gamma + \frac{\mu N}{h}(\cos\beta + \cos\gamma), \tag{41b}$$

If both wheels slip in the free curving region, associated with flanging at the outboard wheel of the lead axle, it follows from equation (41b) that the following transcendental equation governs the yaw angle ψ

$$2h\sin\gamma = \cos\beta + \cos\gamma \tag{42}$$

where β and γ are defined in equations (32b) and (39b). Once ψ is determined, the flange force F_{g_2} follows from (41) and the axle forces from (39a).

If both wheels slip in the constrained curving region, defined by (37) then equations (41a) and (39a) are used to find the flange forces and axle forces, respectively.

Results based on these equations are shown in Figures 4-6 and it is seen that the wheel slip condition has a dramatic effect on flange forces and wheel/rail forces. Results are presented for both $\mu = 1/2$ and $\mu = 1$; the latter value leads to the maximum possible force levels with lead axle flange and wheel/rail forces remaining about twice the force levels associated with $\mu = 1/2$. Although the lead axle wheels slip in the free curving region, the trailing axle wheels do not slip until the constrained curving region is reached. Once slipping occurs on both axles, the wheel/rail forces on the leading axle level off and start to decrease with increasing curvature, as shown in Figure 5. The forces on the outboard wheel (flanging) are about twice the forces on the inboard wheel. The wheel/rail forces on the trailing axle (Figure 6, $\mu = 1/2$) follow a similar pattern. The forces on the inboard wheel (flanging) are greater than the forces on the outboard wheel. Through a large range the lead axle forces are greater than the trailing axle forces. At 333 feet (101.5 meters) the outboard and inboard wheel/rail forces for the leading axle are -12,275# and 6,765#, respectively while the corresponding wheel/rail forces at the trailing axle are -432# and 6,065#. The flange force (Figure 4) on the lead axle F_{g_2} shows a pattern of leveling off and decreasing for $\mu = 1/2$; however, the trailing axle flange force F_{g_1} continues to grow with curvature. For a radius of 500 feet (152.4 meters) and $\mu = 1/2$, $F_{g2} = -17,000\#$ and $F_{g_1} = 0$ while at a radius of 250 feet (76.2 meters), $F_{g_2} = -17,530\#$ and $F_{g_1} = 9,120\#$. Finally these wheel slip results for $\mu = 1/2$ at a radius of 850 feet (250 meters) are shown in Figure 3 in parentheses. Since the onset of slipping occurs at about 1150 feet for $\mu = 1/2$, these force levels for the 850 foot radius are considerably below the non-slipped values shown in Figure 3.

4. NONLINEAR CREEP RELATIONS

The previous analyses assumed a linear relation between creep velocity and creep force, for the wheel without slipping, and further assumed that the creep coefficients were the same for all wheels. To obtain a more realistic force condition, it is now assumed that the resultant creep force at each wheel is non-linearly related to the resultant creep velocity. The creep forces and moments from equations (6) and (7) now become

$$F_1 = -2f_1\left(\frac{h\ell}{R} - \psi\right) + F_{g_1}$$
$$F_2 = 2f_2\left(\frac{h\ell}{R} + \psi\right) + F_{g_2} \tag{43a}$$

$$M_1 = -2f_1\ell\left[\frac{\alpha}{r_o}(y - h\ell\psi) - \frac{\ell}{R}\right]$$
$$M_2 = -2f_2\ell\left[\frac{\alpha}{r_o}(y + h\ell\psi) - \frac{\ell}{R}\right] \tag{43b}$$

where f_1 and f_2 refer to the creep coefficients on the trailing and leading axles, respectively. In addition, it has been assumed that as a first approximation, the creep coefficients for pure lateral and pure longitudinal motion are equal. Setting both the total lateral force and total truck moment to zero, leads to two equations which can be solved for explicit expressions for the flange forces F_{g_1} and F_{g_2}.

$$F_{g_2} = -\frac{(f_1+f_2)}{h}\left[\frac{\ell}{R} - \frac{\alpha y}{r_o}\right] - \frac{\alpha\ell}{r_o}\psi(f_1-f_2) - 2f_2\left(\frac{h\ell}{R}+\psi\right) \tag{44a}$$

$$F_{g_1} = \frac{(f_1+f_2)}{h}\left[\frac{\ell}{R} - \frac{\alpha y}{r_o}\right] + \frac{\alpha\ell}{r_o}\psi(f_1-f_2) + 2f_1\left(\frac{h\ell}{R}-\psi\right). \tag{44b}$$

Using the relations from equations (43) and (44) a complete analysis of the steady state curving problem can be carried out to describe fully the geometric and loading characteristics for the regions of creep guidance, free curving and constrained curving. However, complete details are given only for the free curving region and a numerical comparison is provided for an 850 foot radius. For this free curving region, the outboard wheel of the leading axle is flanging and the appropriate relations are given in equations (17) and (35). Setting the flange force for the trailing axle to zero in equation (44b) leads to an expression for the yaw angle.

$$\psi = \frac{\left[\frac{f_1+f_2}{2f_1} + h^2\right]\frac{\ell}{R} - \frac{1}{2}\left(\frac{f_1+f_2}{f_1}\right)\frac{\alpha q}{r_o}}{h\left(1 - \frac{\alpha\ell}{r_o}\right)} \tag{45}$$

$\psi_{max} = q/h\ell.$

This equation for ψ and ψ_{max} reduces to equation (18) when $f_1 = f_2$ and $P = 0$. The flange force F_{g_2} can be obtained by substituting yaw angle from (45) into equation (44a).

The nonlinear creep relations, which are derived from the work of Johnson and Vermuellen, follow the form derived by Cooperrider, Ref. [8] and is depicted in Figure 7. The relationship involves the resultant wheel force F_R and the resultant creepage V_R in the form*

$$\frac{F_R}{\mu N} = (f^*V_R) - \frac{1}{3}(f^*V_R)^2 + \frac{1}{27}(f^*V_R)^3 \qquad V_R < \frac{3}{f^*}$$

$$\frac{F_R}{\mu N} = 1 \qquad V_R > \frac{3}{f^*}. \tag{46}$$

When the relationship between the resultant force and resultant creepage has been established from equation (46), an <u>equivalent linearization</u> can be determined (as shown in Figure 7 by drawing a straight line from the origin to the appropriate point on the non-linear F_R vs. V_R curve) from the relation

$$f = F_{R/V_R}. \tag{47}$$

The coefficient f* used in the non-linear relationship of (46) is found after fixing μ, the friction coefficient. For example, setting $\mu = 0.5$ and assuming that an approximate value of the creep coefficient is 150 times the wheel load N, leads to the relation

$$\mu N f^* = 150\frac{W}{8}$$

$$f^* = \frac{150}{\mu} \tag{48}$$

$$= 300.$$

The creep relation from equation (46) then becomes (a 100,000# car body has been assumed),

$$\frac{F_R}{6250} = 300V_R - \frac{1}{3}(300V_R)^2 + \frac{1}{27}(300V_R)^3 \qquad V_R < .01$$

$$F_R = 6,250 \qquad V_R \geq .01 \tag{49}$$

where the resultant creepage for wheels on the leading and trailing axles, are

*Creepage is defined as the creep velocity normalized by V, the forward velocity of the truck.

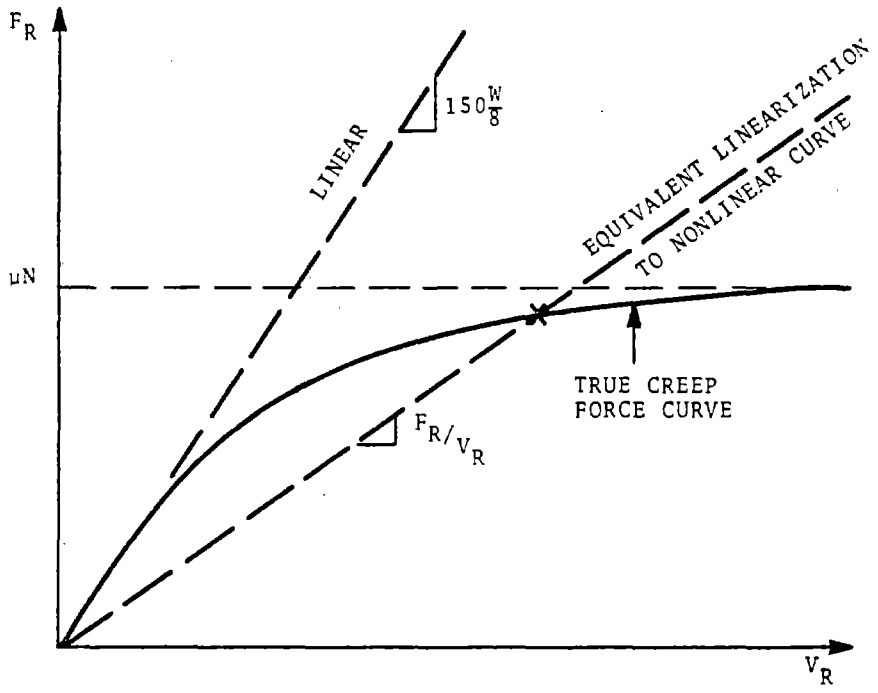

FIGURE 7. NONLINEAR CREEP FORCE RELATIONSHIP AND EQUIVALENT LINEARIZATION

$$V_{R_2} = \sqrt{\left(\frac{h\ell}{R} + \psi\right)^2 + \left(\frac{\alpha q}{r_o} - \frac{\ell}{R}\right)^2}$$

$$V_{R_1} = \sqrt{\left(\frac{h\ell}{R} - \psi\right)^2 + \left(\frac{\alpha}{r_o}\{q - 2h\ell\psi\} - \frac{\ell}{R}\right)^2}, \qquad (50)$$

Since ψ, as defined in equation (45) is a function of the creep coefficients f_1 and f_2, an iterative calculation must be performed for the force - velocity relation of (49) until the results converge and the proper creep coefficients are determined from (47).

For the 850 foot radius curve discussed previously, the creep coefficients acting at the wheels of the leading and trailing axles are calculated as

$$f_2 = 0.633 \times 10^6 \#$$

$$f_1 = 1.3634 \times 10^6 \#, \qquad (51)$$

It is of interest to note that the initial estimate of creep coefficient from equation (27), $f = 75\ W/8$ ($f = 9.375 \times 10^5 \#$) in the linear creep calculation, is an approximate average of the creep coefficients for the leading and trailing axles from equation (51). Once the creep coefficients are known, the forces can be found from equation (43) and (44). At 850 feet, the flange force on the lead outer wheel is

$$F_{g_2} = -15,708\# \qquad (52)$$

which is about 75% of the flange force predicted in equation (28) by the linear theory without slipping and quite close to the 14,893# flange force predicted in equation (34a) for the linear theory including wheel slip. The lateral wheel rail forces can also be calculated and compared to the linear results at 850 feet shown in Figure (3),

leading axle outboard

$$= F_{g_2} + f_2\left(\frac{h\ell}{R} + \psi\right) - \frac{W}{8}\alpha$$

$$= -10,162\# \qquad \left[\begin{matrix}\text{LINEAR INCLUDING} \\ \text{Slip} \\ -9,341\#\end{matrix}\right] \qquad (53)$$

leading axle inboard

$$= f_2\left(\frac{h\ell}{R} + \psi\right) + \frac{W}{8}\alpha \qquad \left[\begin{matrix}\text{LINEAR INCLUDING} \\ \text{Slip} \\ 6,802\#\end{matrix}\right]$$

$$= 6,796\#$$

trailing axle outboard, inboard

$$= -f_1 \left(\frac{h\ell}{R} - \psi\right) - \frac{W}{8}\alpha \qquad \begin{bmatrix}\text{LINEAR INCLUDING} \\ \text{Slip}\end{bmatrix}$$

$$= \begin{matrix}1058^{\#} \\ 2308^{\#}\end{matrix} \qquad \begin{matrix}631^{\#} \\ 1881^{\#}\end{matrix}.$$

The results based on the nonlinear creep relations are superimposed on the linear creep theory and plotted in Figures 8 and 9. The nonlinear creep calculations are carried out until saturation occurs on the wheels of the leading axle, $F_{R_2} = \mu N$. As is shown on the Figures, the nonlinear creep results are bracketed by the linear creep results for f = 75W/8 and 150W/8. In Figure 9, the nonlinear creep results merge almost perfectly with the wheel/rail force for $f = .9375 \times 10^6$# at the inboard (non-flanging) wheel as the saturation level is reached at the wheel slip condition. The wheel/rail force at the lead outboard wheel is slightly greater for the nonlinear creep theory in both the non-slip and slipped region. As shown in Figure 8, the flange force at the lead outboard wheel approaches the linear slipped results from below.

CONCLUSIONS

Results have been presented in closed form for the forces generated in steering a rigid truck through a curve under steady state conditions. These wheel/rail forces and flange forces are derived for a wheel geometry modeled by conical wheel treads with vertical flanges. These results are expected to provide a good approximation for the forces acting on more realistic wheel profiles as long as wheel climb does not predominate in the response. Three curving regions are identified, creep guidance, free curving (flanging on lead outer wheel), and constrained curving (flanging on lead outer wheel and trailing inner wheel). The analysis includes both linear and nonlinear creep theory and also includes the effect of force saturation and wheel slip. Some simple suggestions are given for estimating the creep coefficient in a linear creep theory so that the force levels predicted are quite close to the forces calculated from the more complicated nonlinear creep theory. It is shown that force saturation and wheel slippage greatly affect the force levels.

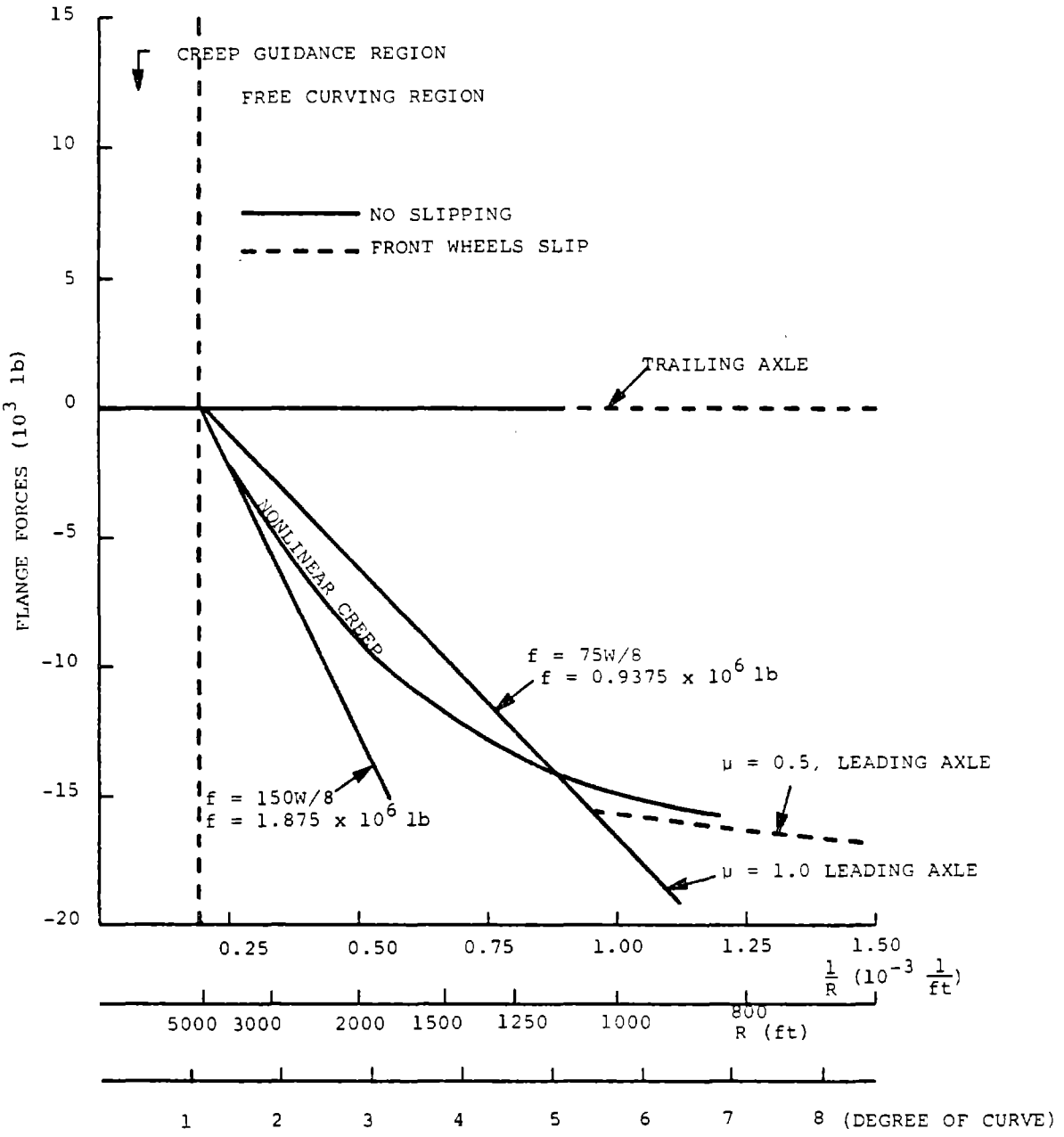

FIGURE 8. FLANGE FORCE VERSUS RADIUS. COMPARISON OF LINEAR AND NONLINEAR CREEP CALCULATION

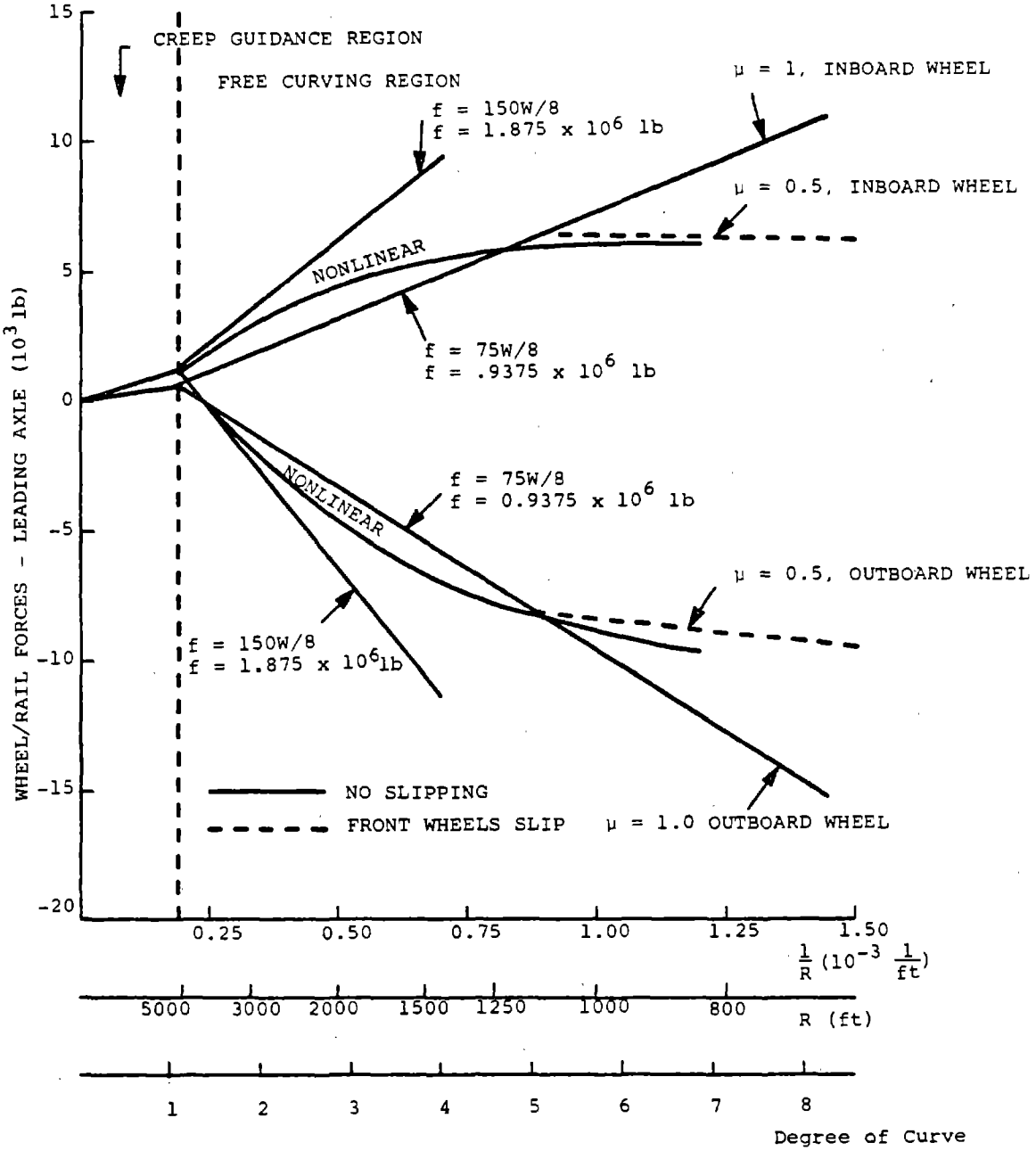

FIGURE 9. WHEEL/RAIL FORCE ON LEADING AXLE VERSUS RADIUS. COMPARISON OF LINEAR AND NONLINEAR CREEP CALCULATION. (GRAVITATIONAL FORCE NEGLECTED)

5. EFFECTS OF FLANGE FRICTION

In the calculations given above it is assumed that no friction force acts between the flange and the rail. Assuming a value for the coefficient of friction μ_F between flange and rail as shown in Figure 10, the lateral force balance and moment relations of equations (9) and (10) are

$$4f\psi + (Fg_1 + Fg_2) + P = 0$$

$$4f\ell\left[\frac{\ell}{R} - \frac{\alpha y a}{r_o}\right] + 4f\,\frac{h^2\ell^2}{R} + (Fg_2 - Fg_1)h\ell + (Fg_2 + Fg_1)\mu_F\ell = 0. \tag{54}$$

Solving these equations for flange force gives

$$Fg_2 = -\frac{2f}{h}\left[\frac{(1+h^2)\ell}{R} - \frac{\alpha y a}{r_o}\right] + \left(\frac{P}{2} + 2f\psi\right)\left(\frac{\mu_F}{h} - 1\right)$$

$$Fg_1 = \frac{2f}{h}\left[\frac{(1+h^2)\ell}{R} - \frac{\alpha y a}{r_o}\right] - \left(\frac{P}{2} + 2f\psi\right)\left(\frac{\mu_F}{h} + 1\right) \tag{55}$$

which shows that the magnitude of the flange force is reduced by the presence of friction μ_F.

The effects of μ_F on the three curving regions are found from these equations. In the creep guidance region the flange forces are zero so that all the relations for yaw angle, axle force and wheel/rail force remain the same as shown in equations (13)-(16a). In the free curving region, the trailing flange force is zero, which leads to

$$\psi = \frac{(1+h^2)\frac{\ell}{R} - \frac{\alpha q}{r_o} - \frac{Ph}{4f}\left(\frac{\mu_F}{h} + 1\right)}{h\left(1 - \frac{\alpha\ell}{r_o} + \frac{\mu_F}{h}\right)} \tag{56}$$

and shows that the yaw angle is reduced by the presence of flange friction. The flange force Fg_2 follows immediately from equation (55)

$$Fg_2 = -4f\psi - P$$

$$= -\frac{4f}{h}\left[\frac{(1+h^2)\frac{\ell}{R} - \frac{\alpha q}{r_o}}{\left(1 - \frac{\alpha\ell}{r_o} + \frac{\mu_F}{h}\right)}\right] + \frac{P\,\frac{\alpha\ell}{r_o}}{\left(1 - \frac{\alpha\ell}{r_o} + \frac{\mu_F}{h}\right)} \tag{57}$$

which is identical in form to equation (19). In the constrained curving region the yaw angle reaches its maximum value

$$\psi = q/h\ell \tag{58}$$

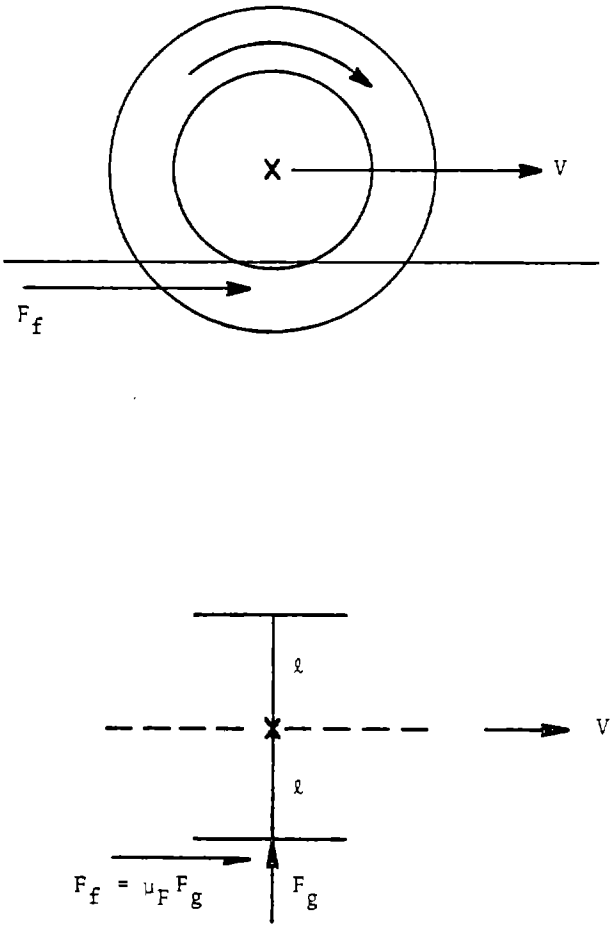

FIGURE 10. FLANGE FORCE AND FRICTION FORCE DUE TO FLANGE FRICTION

and the flange forces follow from (55)

$$Fg_2 = -\frac{2f}{h}\left[(1+h^2)\frac{\ell}{R}\right] + \left(\frac{P}{2} + \frac{2f}{h\ell}\,q\right)\left(\frac{\mu_F}{h} - 1\right)$$

$$Fg_1 = \frac{2f}{h}\left[(1+h^2)\frac{\ell}{R}\right] - \left(\frac{P}{2} + \frac{2f}{h\ell}\,q\right)\left(\frac{\mu_F}{h} + 1\right). \tag{59}$$

As an indication of the effect of flange friction, the flange force and lateral wheel force at the outboard wheel of the leading axle are calculated for the free curving region, with zero centrifugal force (P=0). The flange force is

$$Fg_2 = -\frac{4f}{h}\left[\frac{(1+h^2)\frac{\ell}{R} - \frac{\alpha q}{r_o}}{\left(1 - \frac{\alpha\ell}{r_o} + \frac{\mu_F}{h}\right)}\right] \tag{60}$$

and wheel/rail force is (equation (20))

$$= Fg_2 + f\left(\frac{h\ell}{R} + w\right) - \frac{W}{8}\alpha \tag{61}$$

$$= \frac{3}{4}\,Fg_2 + \frac{fh\ell}{R} - \frac{W}{8}\alpha. \qquad \text{leading axle outbound}$$

The calculations are done for conditions listed on Figure 3 at R = 850 feet, for various values of the coefficient of friction μ_F. The results are given in Table 2 and show that flange friction has a significant effect. A flange with friction coefficient μ_F = .4 reduces the flange force by 24% from the lubricated flange result (μ_F=0). The corresponding reduction for the wheel/rail force at the lead outer wheel is 30%.

TABLE 2. EFFECT OF FLANGE FRICTION ON FORCES IN FREE CURVING REGION, LINEAR CREEP THEORY ($f = 9.375 \times 10^5$ lb, R = 850 ft)

μ_F	Fg_2	W/R FORCE AT LEAD OUTER WHEEL
	lb	lb
0	-20,282	-12,182
.2	-17,537	-10,123
.4	-15,445	-8,548
.6	-13,800	-7,320
.8	-12,472	-6,324
1.0	-11,377	-5,505

6. INFLUENCE OF TRUCK FLEXIBILITY ON CALCULATED WHEEL/RAIL FORCES

In actual truck designs the interaction between the truck axles is through the elastic members connecting the two axles. The rigid truck represents a limiting case where the stifness of these elastic members is extremely large. An indication of the range of validity of the rigid truck model is obtained from the analysis of flexible trucks conducted in Reference (1) where Newland obtained the minimum radius curve that can be negotiated by a flexible truck with infinite flange clearance and without wheel slip. This relationship is presented by Weinstock (9) in terms of the effective stiffnesses between axles.

$$R \geq \frac{2f_T h\ell}{\mu W} \frac{\left[1 + h^2 \frac{f_L}{f_T}\left\{1 + \frac{\alpha\ell}{r_o}(f_T/K_y h\ell)\right\}^2\right]^{1/2}}{1 + \frac{\alpha\ell}{r_o}\left(f_L f_T/K_y K_\psi\right)} \tag{62}$$

where K_y and K_ψ refer to these effective lateral and yaw stiffnesses. In this equation it is seen that variations in truck stiffness produce negligible changes in the result when:

$$\frac{\alpha\ell}{R_o}(f_T/K_y h\ell) << 1, \quad \frac{\alpha\ell}{r_o}\frac{f_L f_T}{K_y K_\psi} << 1. \tag{63}$$

The rigid truck assumption is therefore expected to be valid for:

$$K_y >> \frac{\alpha f_T}{r_o h}, \quad K_y K_\psi >> \frac{\alpha\ell}{r_o} f_L f_T. \tag{64}$$

For the dimensions used in Figure 3, this leads to:

$$K_y >> 2.4 \times 10^3 \#/\text{inch}$$
$$K_y K_\psi >> 9.4 \times 10^{10} (\#)^2/\text{rad} \tag{65}$$

where both the tangential and lateral creep coefficients are assumed as 1×10^6#. A plot which defines the region of validity of the rigid truck model is shown in Figure 11. For a flexible truck modeled by lateral and longitudinal primary stiffness k_y and k_x connected to the frame, relationships may be derived in terms of the effective interaxle stiffness K_y, K_ψ. Following the analyses of Reference (9), it follows that

$$K_\psi = \ell^2 k_x$$
$$K_y = \frac{k_y k_x}{k_x + h^2 k_y} \tag{66}$$

from which the primary stiffness parameters may be written as:

$$k_x = K_\psi/\ell^2$$
$$k_y = K_y/\left(1 - \frac{K_y}{K_\psi} h^2 \ell^2\right) \tag{67}$$

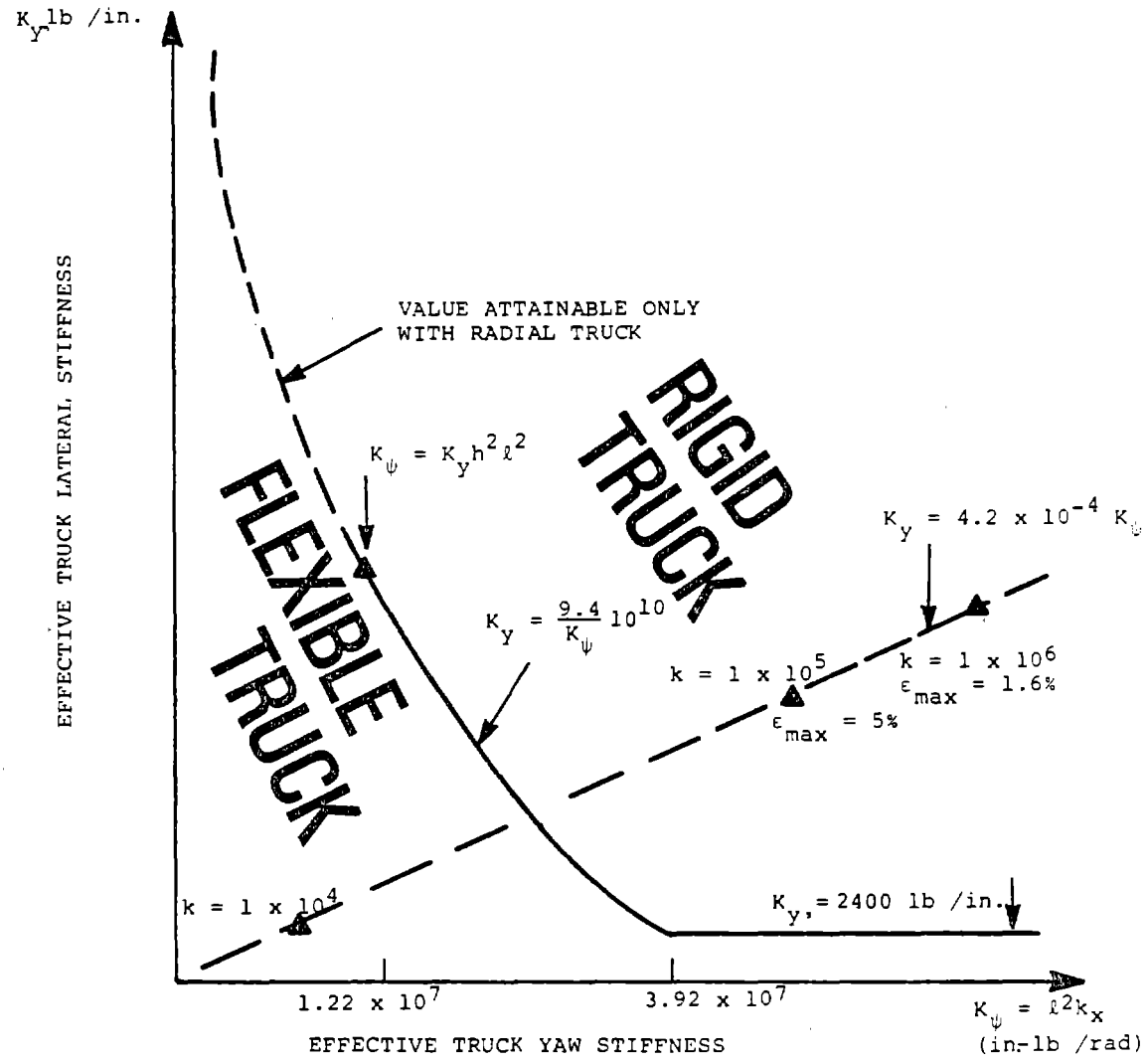

FIGURE 11. RANGE OF VALIDITY OF FLEXIBLE AND RIGID TRUCK MODELS IN TERMS OF EFFECTIVE INTERAXLE STIFFNESS (α = 0.05, h = 1.41)

where the vanishing of the denominator ($K_\psi = K_y h^2 \ell^2$) defines the boundary between radial and conventional truck models. Inequalities defining the rigid truck range can then be defined based on the results in equation (65) and the parameters listed in Figure (3) (h = 1.41, ℓ = 28.2")

$$k_y \geq \frac{k_x}{8.46 \times 10^{-9} k_x^2 - 2} \qquad 15{,}400 < k_x < 49{,}250\#/\text{inch}$$

$$k_y \geq \frac{2400}{1 - (4800/k_x)} \qquad 49{,}250\#/\text{in} < k_x \tag{68}$$

A plot defining the range of validity of the rigid truck model in terms of primary stiffness is shown in Figure (12).

As an indication of the range of validity of the rigid truck results, a parametric study is made of a flexible truck using the Battelle steady state curving program SSCUR(7). For a two-axle flexible truck with equal primary stiffnesses of

$$k_x = k_y = 1 \times 10^4 \#/\text{inch} \tag{69}$$

runs were made with these stiffness values and then subsequent runs were made as the stiffness values are increased by factors of ten. Defining k as the value of these equal primary stiffnesses, equation (66) can be written as:

$$K_\psi = \ell^2 k$$

$$K_y = \frac{k}{1 + h^2}. \tag{70}$$

The lateral wheel/rail forces computed by the steady state curving program are plotted against this "stiffness factor" in Figure 13 along with the forces for the rigid truck model in the free curving region (flanging on the lead outer wheel). For the case of stiffness factor = 1, corresponding to the values in equation (69), the inequalities of equations (65) and (68) are not satisfied and the rigid truck results cannot be used to predict force. (The flexible truck for this value of primary stiffness actually flanges on the outer wheel of both the leading and trailing axle.) Increasing the primary stiffness by a factor of 10, the stiffness inequalities of equations (65) and (68) are satisfied, and the comparison with the rigid truck is excellent. Both the flexible truck and the rigid truck predict flanging on the lead outer wheel with the wheel/rail forces comparing to within 5% while the force at the lead inboard wheel compares to within 2.5%. For an increase in the stiffness factor by another factor of 10, the forces are within 1.6% as shown in Figure (13). The results in this parametric comparison study are also shown in Figure (11). From equation (70), it follows that

$$K_y = K_\psi / \ell^2 (1 + h^2)$$

$$= 4.2 \times 10^{-4} K_\psi \tag{71}$$

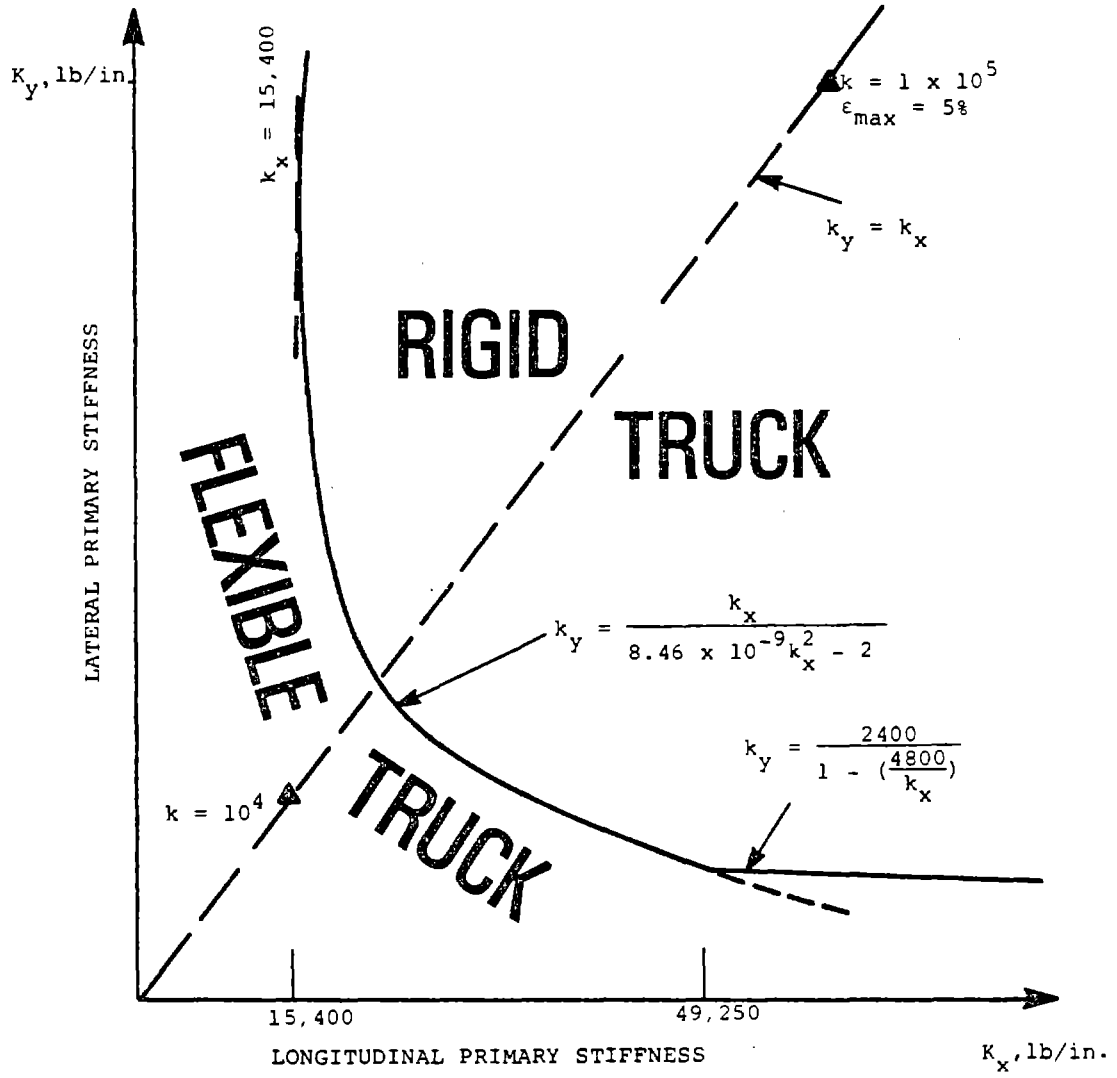

FIGURE 12. RANGE OF VALIDITY OF FLEXIBLE AND RIGID TRUCK MODELS IN TERMS OF PRIMARY STIFFNESS (h = 1.41, ℓ = 28.2", α = 0.05)

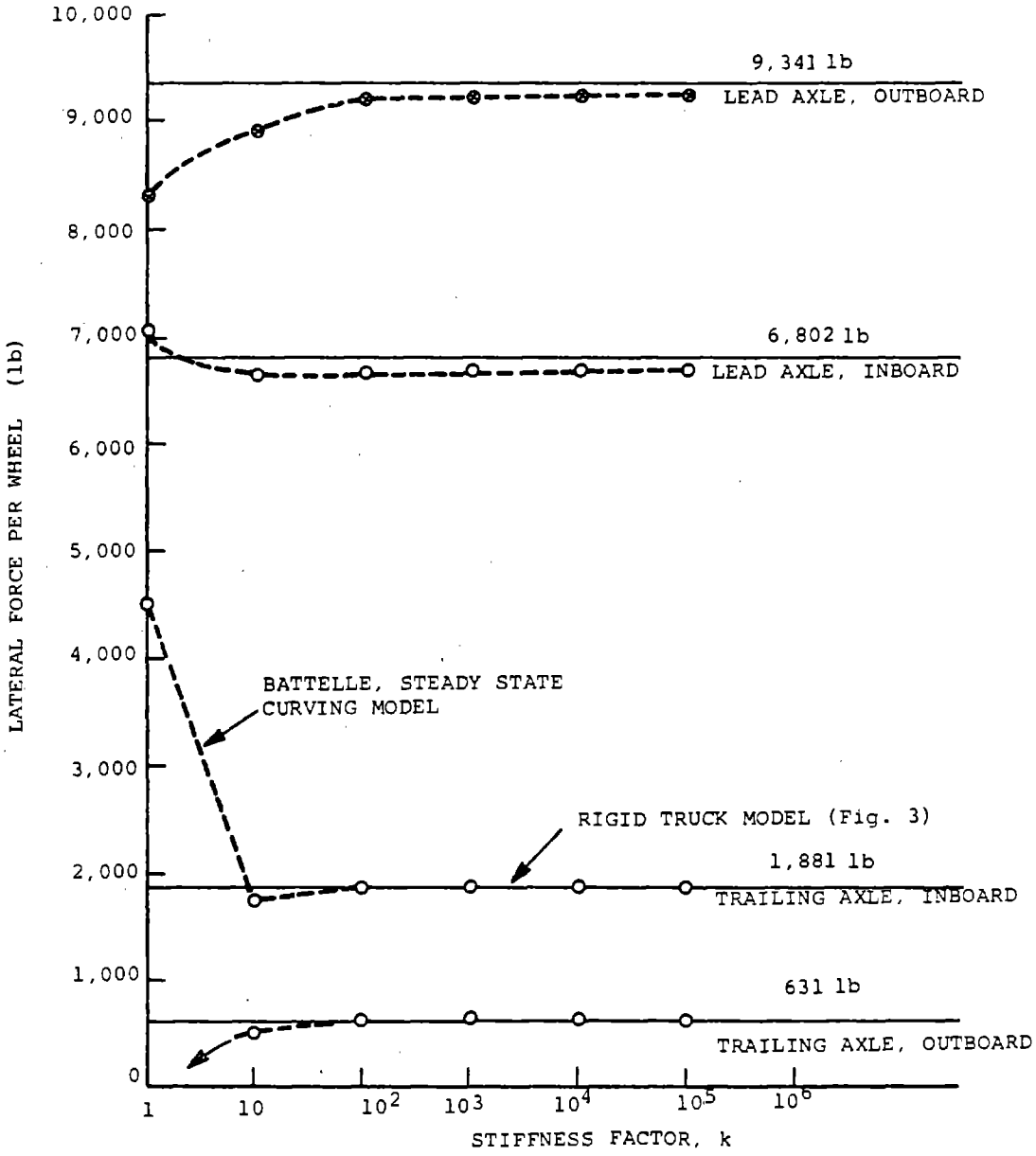

FIGURE 13. COMPARISON OF BATTELLE STEADY STATE CURVING MODEL TO A RIGID TRUCK

for the case of equal primary stiffness k. This linear relationship between effective lateral and yaw stiffness is shown in Figure (11). Similar results of the parametric study are shown in Figure 12.

7. COMPARISON OF RIGID TRUCK RESULTS WITH TEST DATA

The rigid truck results provide closed form relationships for estimating the wheel/rail forces, angle of attack and sliding conditions during steady state curving. This type of information is useful for the design and evaluation of field tests and an initial evaluation of expected wheel/rail forces. An example of this combined testing and analytical approach is given in Ref. [10] for the Washington Metropolitan Area Transit Authority investigation of possible wear problems during transit operations on curves. The track was instrumented so that wheel/rail forces could be recorded and flange forces calculated.

The truck suspension stiffness for this transit truck is estimated as

$$k_x = 160{,}000\#/\text{inch (longitudinal)}$$
$$k_y = 23{,}000\#/\text{inch (lateral)}. \tag{72}$$

Since the longitudinal primary stiffness is in the range $k_x >> 49{,}250\#/\text{inch}$, the truck parameters are in the rigid range as defined by equation (68),

$$k_y >> 2{,}474\#/\text{inch} \qquad k_x >> 49{,}250\#/\text{inch}. \tag{73}$$

A calculation of the effective interaxle stiffness from equation (66),

$$K_\psi = \ell^2 k_x$$
$$= 1.27 \times 10^8 \text{ in-\#/rad}$$
$$K_y = \frac{k_y k_x}{k_x + h^2 k_y} \tag{74}$$
$$= 1.79 \times 10^4 \#/\text{inch}$$

also verifies that the truck parameters are in the rigid range based upon the limits set by equation (65).

Tests were run with trucks equipped with cylindrical wheels and also for trucks with conical wheels. Measurements of wheel/rail forces were made with strain gages mounted on the high rail and the low rail of the Washington Metro at an 800 foot radius curve located near Washington National Airport for speeds ranging from 5 - 40 mph. For a wheel rail friction coefficient of 0.5 and a flange friction coefficient of 0.4 the wheel rail force predicted by the rigid truck analysis is 6,200 lb compared to the measured force of 6,460 lb (averaged over all runs for dry rail conditions at the maximum force location) reported in Reference 10. The flange force predicted by the rigid truck analysis is 12,100, which compares well with the 11,790 lb obtained from the measured data.

8. REFERENCES

1. Newland, D.E., "Steering a Flexible Railway Truck on Curved Track," Journal of Engineering for Industry, Transactions of ASME, Vol. 91, Series B, No. 3, August 1969, p. 908-918.

2. Boocock, D., "The Steady State Motion of Railway Vehicles on Curved Track," Journal of Mechanical Engineering Science, Vol. 11, No. 6, 1969, p. 556-566.

3. Koffman, J.L., "Running Through Curves," The Railway Gazette, April 21, 1967, p. 307-311.

4. Koci, L.F. and Marta, H.A., "Lateral Loading Between Locomotive Truck Wheels and Rails Due to Curve Negotiation," ASME Paper No. 65-WA/RR-4, 1965.

5. Perlman, A.B., "Computational Methods for the Prediction of Truck Performance in Curves," ASME Paper No. 76-WA/RT-15, 1976.

6. Elkins, J.A. and Gostling, R.J., "A General Quasi-Static Curving Theory for Railway Vehicles," Presented at the International Union of Theoretical and Applied Mechanics Symposium on the Dynamics of Vehicles on Roads and Tracks, Vienna, September 1977.

7. Ahlbeck, D., Dean, F., and Prause, R., "A Methodology for Characterization of Wheel Rail Load Environment -- A Pilot Application," Contract No. DOT-TSC-1051, Battelle Columbus (OH) Labs., June 1979. Material on file at DOT-TSC.

8. Cooperrider, N.K., "The Hunting Behavior of Conventional Railway Trucks," Journal of Engineering for Industry, Transactions of ASME, Vol. 94, Series B, No. 2, May 1972, p. 752-762.

9. Weinstock, H., Analyses of Rail Vehicle Dynamics in Support of Development of the Wheel Rail Dynamics Research Facility," Interim Report, DOT-TSC-UMTA-72-10/ UMTA-MA-06-0025-73-2/PB-222-654/6, June 1973.

10. Phillips, C., Weinstock, H., Greif, R., and Thompson, W., "Analysis of Wheel/Rail Forces at the Washington Metropolitan Area Transit Authority," Final Report, DOT-TSC-UMTA-80-25, I/UMTA-MA-06-0025-80-6, I, June 1980.

110 Copies